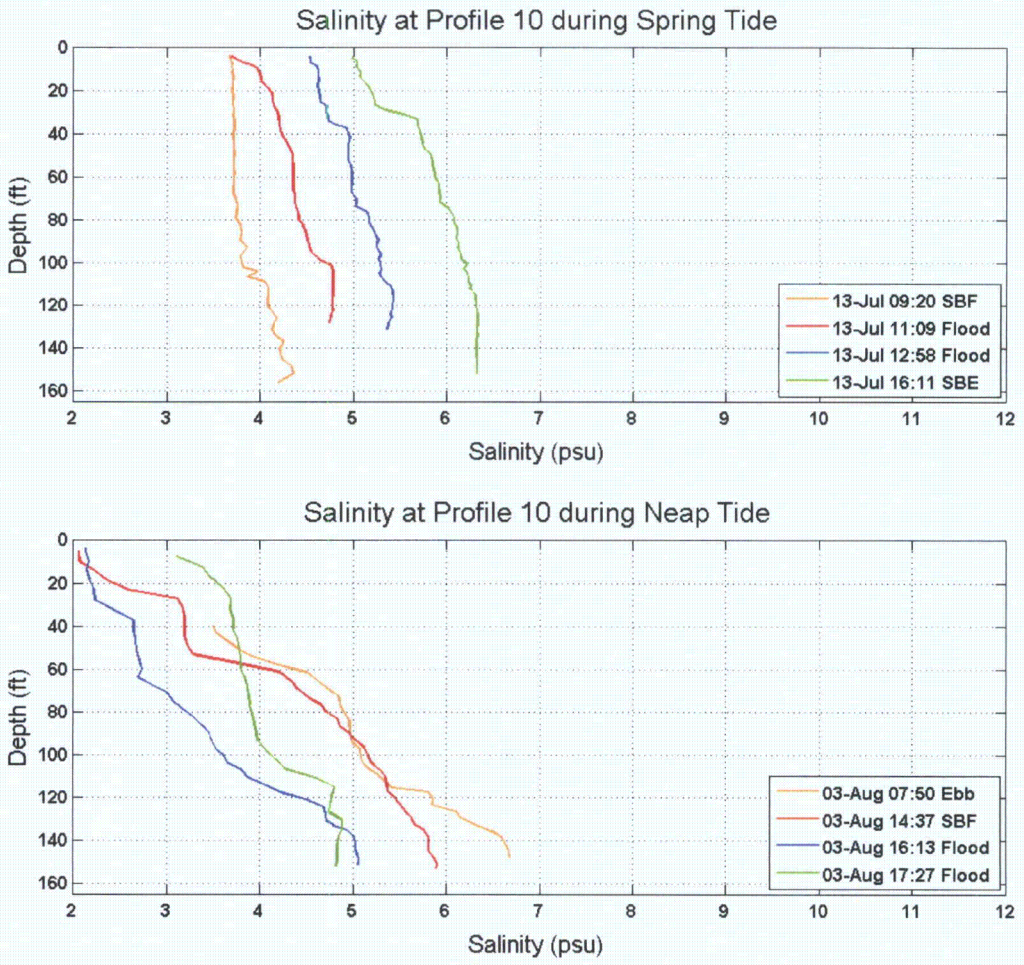

Figure 3-35. Salinity profiles at mobile CTD location 10 on 13 July (upper panel) and 3 August (lower panel..

3.4 CURRENTS

IPEC is located at RM 41.5, north of Haverstraw Bay and just south of a very sharp bend in the River. At IPEC the river is less than 1 mi wide. The channel is deeper on the east side, about 60 ft, and shoals to less than 30 ft on the west side. A stationary ADCP was installed on 8 July at the deeper part of the channel on the east side and was retrieved 68 days later on 14 September. The ADCP recorded data every 5 minutes at 3.3 ft vertical increments over the whole water column, starting at 12.1 ft above the bed.

Both surface and bottom flows are controlled primarily by the tides (with a 12.42 hr period), resulting in a bi-directional flow following the River geometry, generally along a northeast-southwest axis. At this location the surface current was stronger than the bottom current due to bottom friction at the seabed. The current velocities from ADCP Bin 12, approximately 48.2 ft above the seabed, were found to be a

complete record of near surface currents, and thus used as representative of surface currents (Figure 3-36Figure 3-36 and Figure 3-37). At the surface layer (ADCP Bin 12), the maximum peak upstream (flood) velocity was 2.6 ft/s on 10 September, the minimum peak upstream velocity was 0.8 ft/s on 4 August, and the mean peak upstream velocity was 1.6 ft/s. The maximum peak downstream (ebb) velocity was 3.6 ft/s on 9 July, the minimum peak downstream velocity was 1.9 ft/s on 1 September, and the mean peak downstream velocity was 2.6 ft/s. The surface current had a mean downstream component of 0.5 ft/s, resulting in a net speed similar to the River flow. Figure 3-36 also shows the biweekly spring-neap cycle clearly in the ebb (downstream) currents with smaller velocities recurring around 4 August, 19 August, and 2 September.

For the bottom layer, which was taken at approximately 12.1 ft above the seabed (ADCP Bin 1), the maximum peak upstream (flood) velocity was 2.3 ft/s on 8 July, the minimum peak upstream velocity was 1.4 ft/s on 10 July, and the mean peak upstream velocity was 1.7 ft/s. Also for the bottom layer, the maximum peak downstream (ebb) velocity was 2.5 ft/s on 8 September, the minimum peak downstream velocity was 0.1 ft/s on 19 August, and the mean peak downstream velocity was 1.5 ft/s. The mean bottom velocity over the entire period was 0.2 ft/s in the upstream direction, typical of two layer estuarine flow due to the density gradient. The bottom flows show more distinctive spring-neap cycle as the bottom velocity transitions to a small downstream current during early August and September.

The net flow at the surface was in the downstream direction with the strongest flow of 0.5 ft/s. However, the records from the bottom 20 ft at this station had an upstream net flow, with a value ranging between 0.1 and 0.2 ft/s. The cumulative net flow over the whole water column was 1.5 ft/s toward the downstream direction.

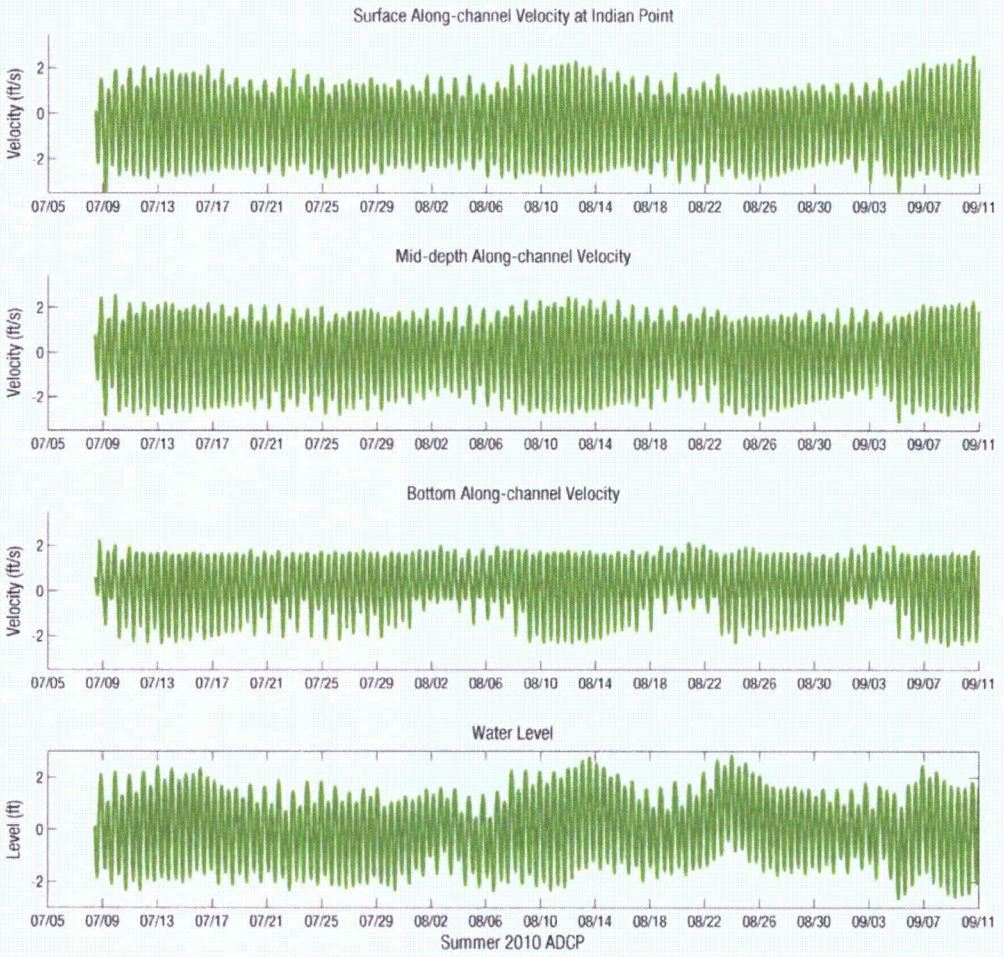

Figure 3-36. Along channel speeds for near surface (upper panel), mid depth (upper middle panel) and near bottom (lower middle panel), and water level (lower panel) at the Indian Point ADCP during the 2010 survey period.

Figure 3-37. Current vector stick plots for near surface (upper panel), mid depth (middle panel) and near bottom (lower panel) at the Indian Point ADCP during the 2010 survey period.

Iona Island is located a little over 3 miles North of Indian Point after a hairpin turn in the river (RM 44). In that region, the river is narrow, only 0.3 mi across. An ADCP was located in the deepest part of the channel closer to the east shore, across the river from Iona Island. The ADCP was deployed and retrieved on the same days as the ADCP at Indian Point (8 July to 14 September) and set to the same 5 minute interval recordings and 3.3 ft vertical bins.

Both surface and bottom flows are controlled primarily by the tides (with a 12.42 hr period), resulting in bi-directional flow following the River geometry along a generally northwest-southeast axis. The current velocities from ADCP Bin 26, at approximately 94.16 ft above the seabed, were used as representative of surface currents (Figure 3-38Figure 3-38 and Figure 3-39). For the surface layer, the maximum peak upstream (flood) velocity was 2.8 ft/s on 12 August, the minimum peak upstream velocity was 0.5 ft/s on 4 August, and the mean peak upstream velocity was 1.9 ft/s. Also for the surface layer, the maximum peak downstream (ebb) velocity was 3.0 ft/s on 8 September, the minimum peak downstream stream velocity was 1.8 ft/s on 1 September, and the mean peak downstream velocity was 2.5 ft/s. The surface current has a mean downstream component of 0.4 ft/s. Figure 3-38 Figure 3-38 clearly shows the spring-neap tidal cycle in the ebb (downstream) currents, with smallest velocities recurring around 4 August, 19 August, and 2 September.

For the bottom layer (Figure 3-38Figure 3-38), defined as Bin 1 from the ADCP data recording at approximately 12 ft above the seabed, the maximum peak upstream (flood) velocity was 3.2 ft/s on 8 July, the minimum peak upstream velocity was 1.6 ft/s on 31 August, and the mean peak upstream velocity was 2.1 ft/s. Also for the bottom layer, the maximum peak downstream (ebb) velocity was 1.9

ft/s on 8 August, the minimum peak downstream stream velocity was 0.2 ft/s on 4 September, and the mean peak downstream velocity was 1.4 ft/s. The mean bottom velocity over the entire period was 0.5 ft/s upstream, typical of two layer estuarine flow due to the density gradient.

The bottom flows showed a more distinctive spring-neap variation than the surface as the bottom velocity transitions to a small downstream current. The spring-tide velocities have maximum velocities at the surface, nearing 3 ft/s and decrease with depth down to about 1.5 ft/s near the bottom. Neap-tide velocities in general are weaker, and several times during neap cycles, the velocity at the bottom during ebb tides did not in fact ebb, as seen on 2 September.

The bottom flows showed a more distinctive spring-neap variation than the surface as the bottom velocity transitions to a small downstream current. The spring-tide velocities have maximum velocities at the surface, up to 3 ft/s and decrease with depth down to about 1.9 ft/s near the bottom. Neap-tide velocities in general are weaker, and several times during neap cycles the velocity at the bottom during ebb tides did not in fact ebb, as seen on 3 August from the ADCP data. The net flow at the surface layer was in the downstream direction with the strongest residual flow of 0.4 ft/s. However, the records from bottom 12-58 ft above the seabed at this station had an upstream net flow, with a value ranging from 0.1 to 0.5 ft/s. The cumulative flow from the surface to the bottom was 2.1 ft/s in upstream direction.

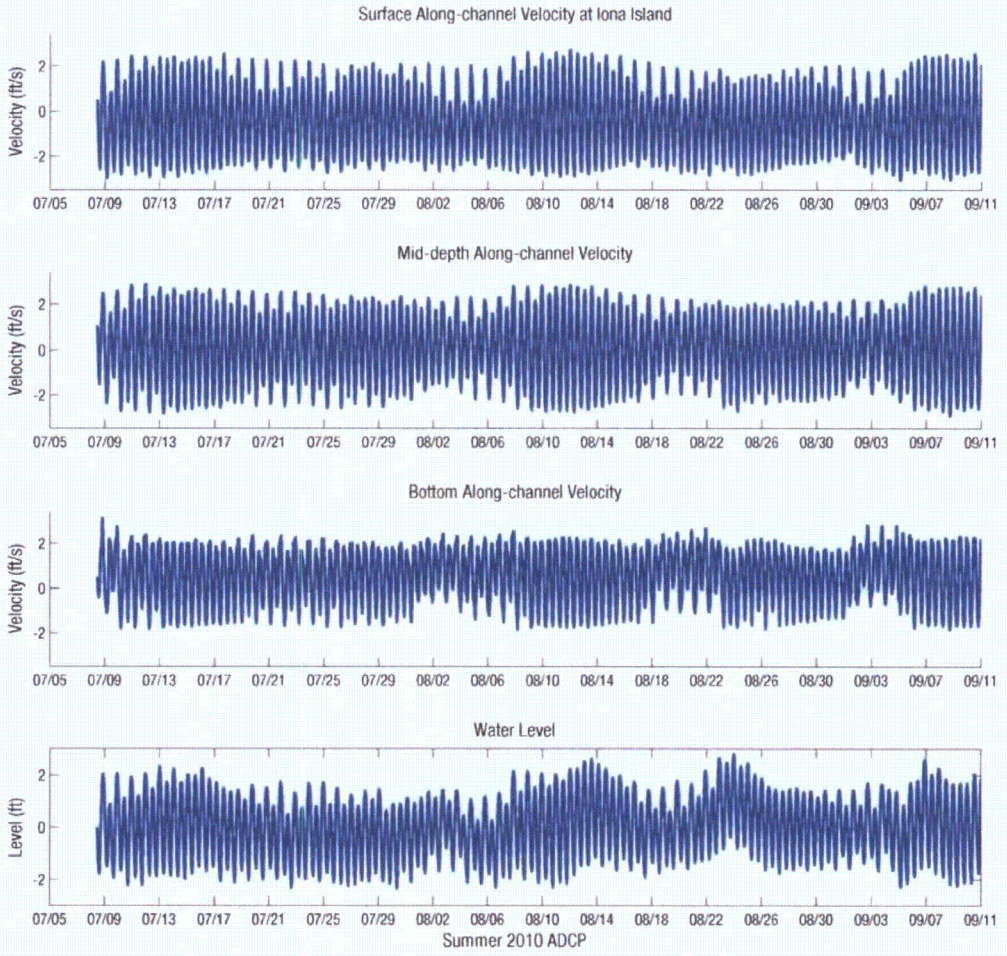

Figure 3-38. Along channel speeds for near surface (upper panel), mid depth (upper middle panel) and near bottom (lower middle panel), and water level (lower panel) at the Iona Island ADCP during the 2010 survey period.

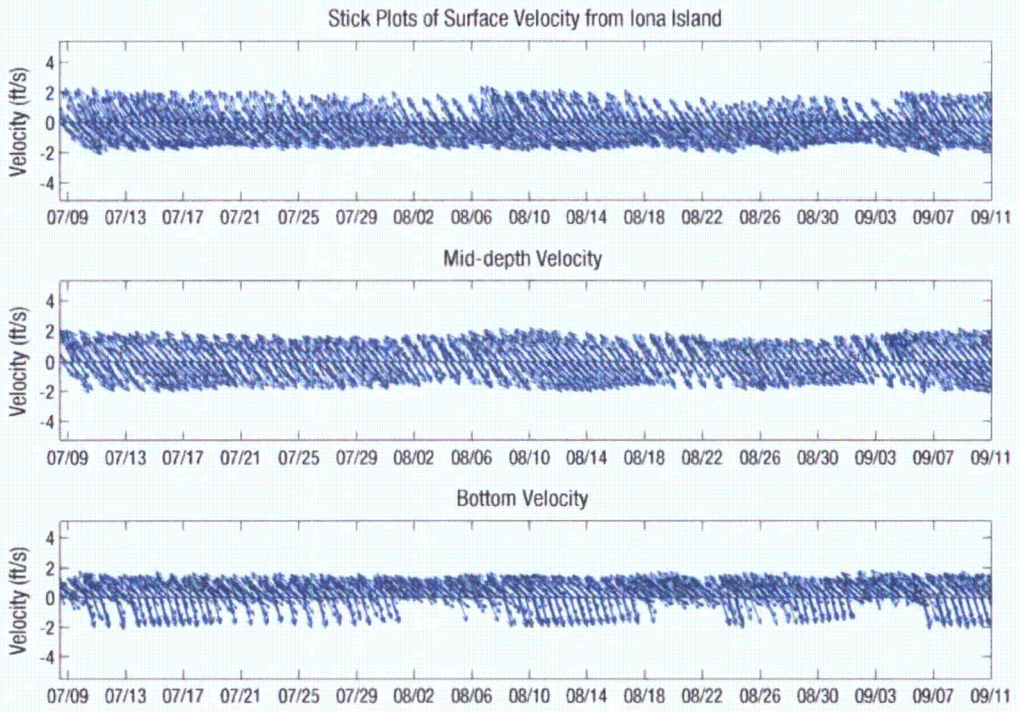

Figure 3-39. Current vector stick plots for near surface (upper panel), mid depth (middle panel) and near bottom (lower panel) at the Iona Island ADCP during the 2010 survey period.

Stony Point is south of Indian Point (near RM 39), in a region where the river width changes drastically. In Haverstraw Bay, where it is very shallow and wide, but the River narrows upstream toward Indian Point. A third ADCP was located closer to the western shore in the deeper part of the channel. The ADCP was deployed on 1 July, several days before the other ADCPs, and retrieved on 14 September.

Both surface and bottom flows were also controlled by the tides with a 12.42 hr period, resulting in a bi-directional flow following the River geometry along a generally northwest-southeast axis. The current velocities from ADCP Bin 16, located approximately 61.5 ft above the seabed, were used as representative of surface currents (Figure 3-40Figure 3-40 and Figure 3-41). For the surface layer, the maximum peak upstream (flood) velocity was 2.7 ft/s on 8 August, the minimum peak upstream velocity was 0.8 ft/s on 4 August, and the mean peak upstream velocity was 1.9 ft/s. Also for the surface layer, the maximum peak downstream (ebb) velocity was 2.7 ft/s on 8 September, the minimum peak downstream stream velocity was 1.7 ft/s on 4 August, and the mean peak downstream velocity was 2.3 ft/s. The surface current had a mean downstream component of 0.2 ft/s.

For the bottom layer (Figure 3-40Figure 3-40), defined as Bin 1 from the ADCP data at approximately 58.6 ft deep, the maximum peak upstream (flood) velocity was 3.0 ft/s on 6 August, the minimum peak upstream velocity was 1.0 ft/s on 3 September, and the mean peak upstream velocity was 2.1 ft/s. Also for the bottom layer, the maximum peak downstream (ebb) velocity was 2.3 ft/s on 11 August, the minimum peak downstream stream velocity was 0.5 ft/s on 3 September, and the mean peak

downstream velocity was 1.6 ft/s. The mean bottom velocity (Bin 1) over the entire period was 0.3 ft/s in the upstream direction.

The net flow at the surface layer was in the downstream direction with the strongest residual flow of 0.2 ft/s. However, the records from bottom 12-42 ft above the seabed at this station had an upstream net flow, with a value ranging 0.1-0.3 ft/s. A cumulative flow from the surface to the bottom was 1.7 ft/s in upstream direction.

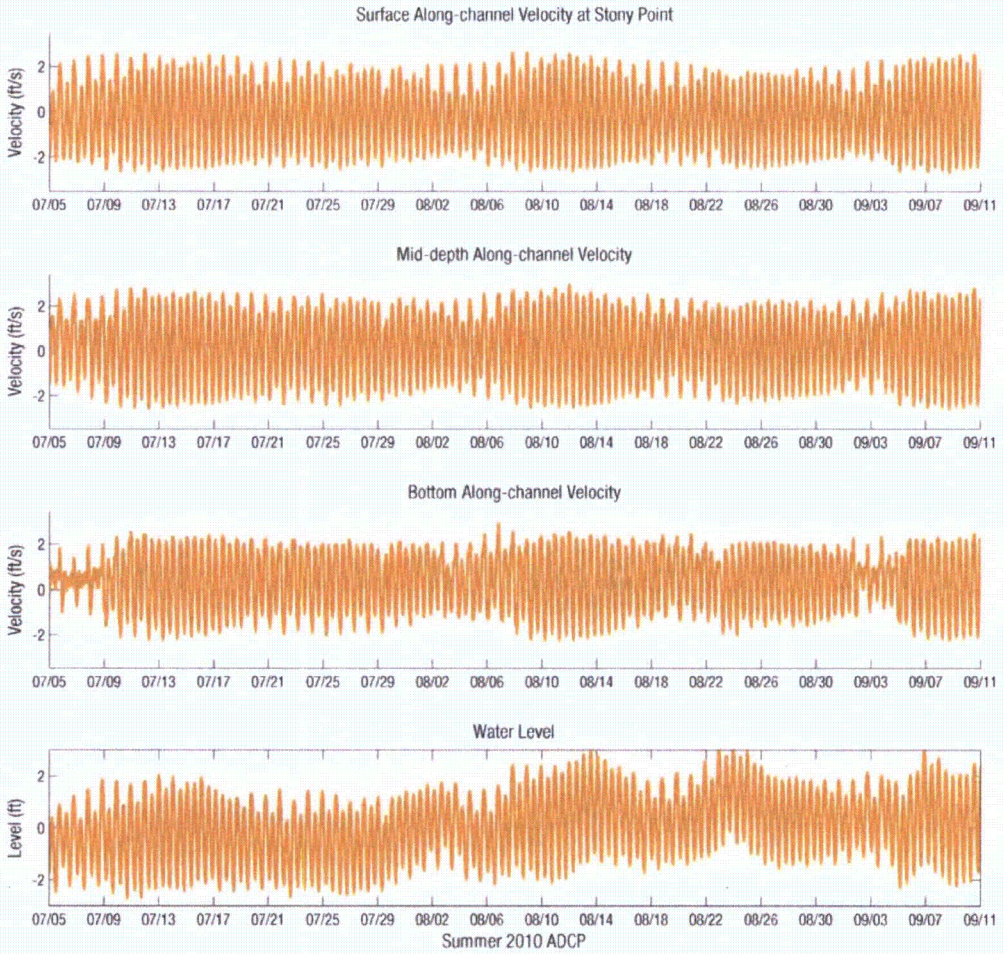

Figure 3-40. Along channel speeds for near surface (upper panel), mid depth (upper middle panel) and near bottom (lower middle panel), and water level (lower panel) at the Stony Point ADCP during the 2010 survey period.

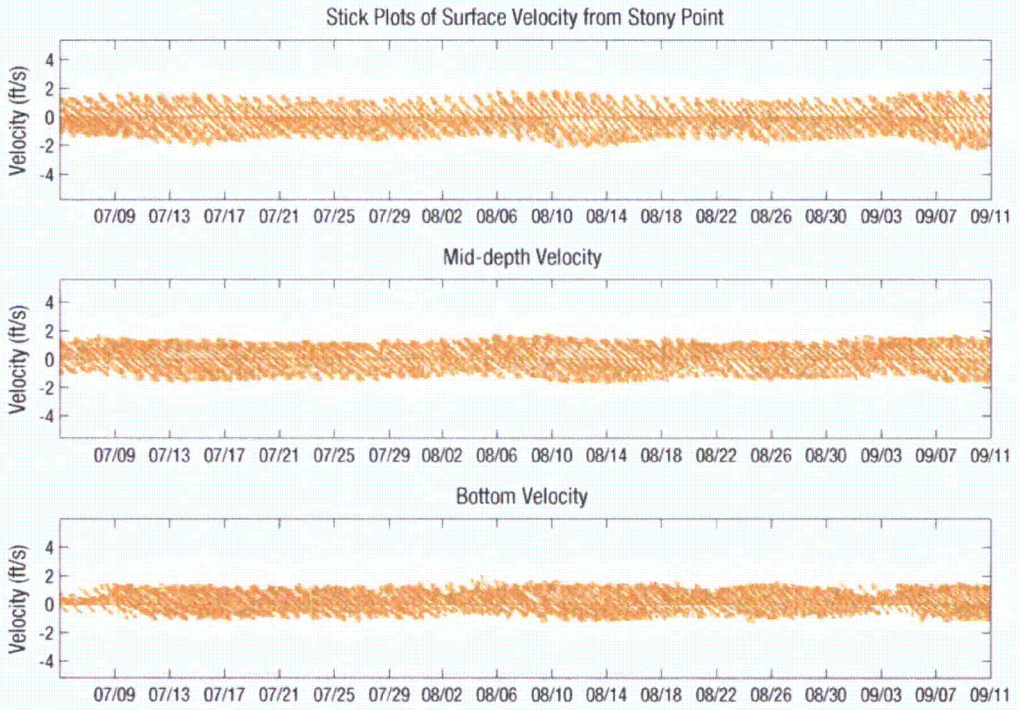

Figure 3-41. Current vector stick plots for near surface (upper panel), mid depth (middle panel) and near bottom (lower panel) at the Stony Point ADCP during the 2010 survey period.

3.5 METEOROLOGY

The Northeast Regional Climate Center (NRCC) database includes historical climate data for the northeastern United States as well as continually updated National Weather Service (NWS) weather observations and forecasts. Data from the NRCC was analyzed for the White Plains Airport, located 18 mi southeast of IPEC.

Meteorological data at White Plains Airport is displayed in Figure 3-42. For the summer 2010 study period, the air temperature at White Plains remained within a range of 53°F to 101°F, with an average of 74.7°F. The dew point generally tracked the air temperature closely, although was typically 10°F to 20°F colder, with an average of 61.1°F. The relative humidity had an average of 65%, with values reaching to 94%. Atmospheric pressure and solar radiation had maximums of 1009.4 mbar and 911.3 W/m^2, respectively, during the study period.

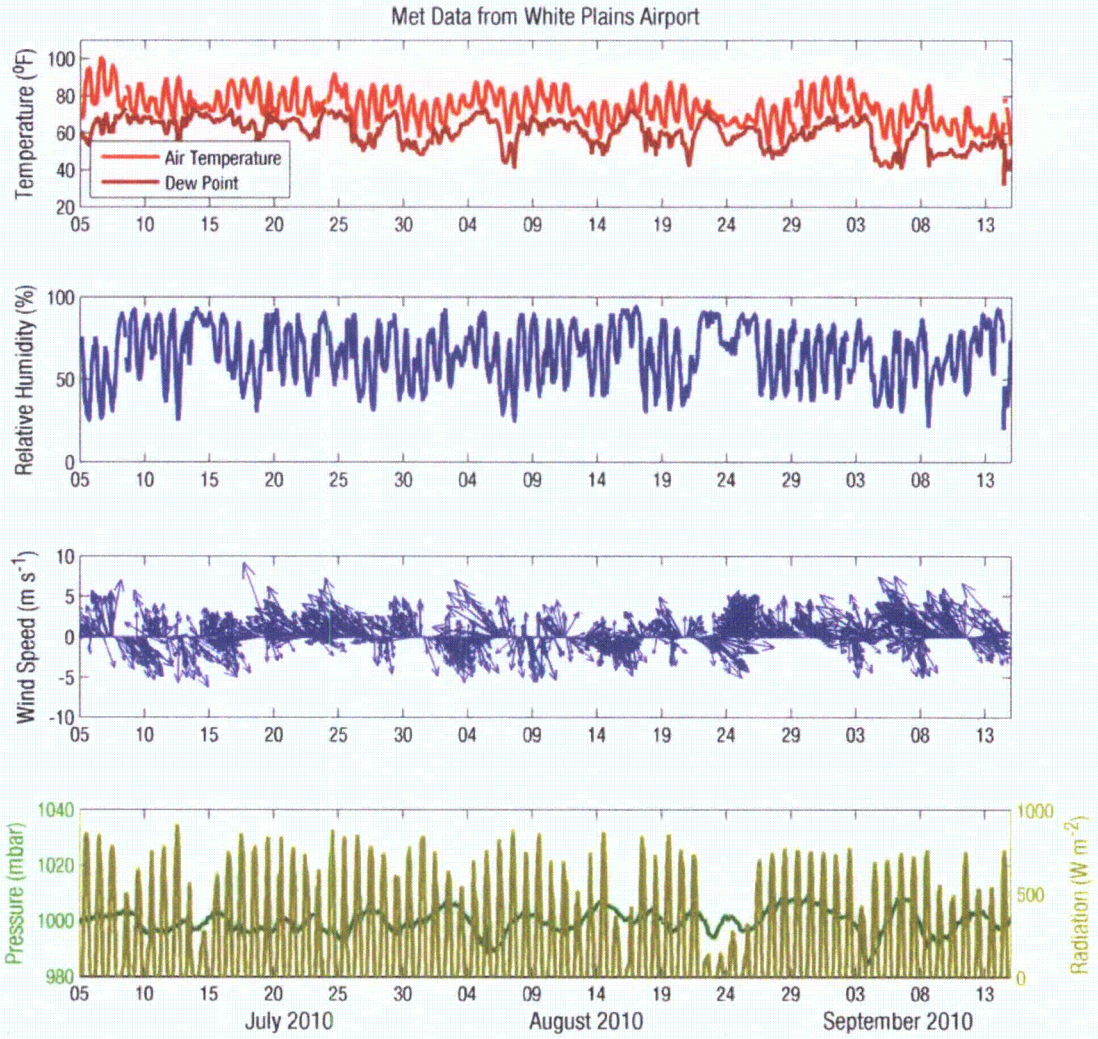

Figure 3-42. Air temperature and dew point (upper panel), relative humidity (upper middle panel), wind speed and direction (lower middle panel), and pressure and radiation (lower panel) during the 2010 survey period at White Plains.

The wind at HPN is displayed as a vector with its length scaled to the speed and its direction pointing downwind (oceanographic convention), as shown in the lower middle panel of Figure 3-42. Wind speeds were under 2.59 m/s for 50% of the time and exceeded 7.2 m/s for 1% of the time during the study period.

3.6 IPEC Plant Operations

IPEC continuously monitors its intake temperature, discharge temperature, and flowrate. Data was provided by IPEC of high resolution (every 20 sec) minimum and maximum temperature measurements denoted as "Avg Intake Temp". Minimum and maximum discharge temperature data was also provided on a 20-sec timestep and denoted as "Avg Dischrg Temp". Discharge flowrate was provided via the Daily

Pump Operation Log in IPEC's *Indian Point Plant Performance Environmental Report* for the months of July and August which provided status information (on or off) for each of the 12 operational circulating water pumps and 17 service water pumps to the minute. All operational circulating water pumps and 13 service water pumps were in service during the July – August period.

The temperature data were first processed to obtain the average of the minimum and maximum on the 20-sec timestep. The data were then averaged with a centered 1-hr filter and subsampled to the hour to be consistent with the other data sets. The discharge flowrate data were converted to an hourly value by averaging each individual pump flowrate over an hour based on its minute-by-minute status (on or off) and then adding the flows from the 25 active pumps.

The time series of IPEC operational data during the July to mid August period is shown in Figure 3-43. Discharge flow, shown in the upper panel, was relatively constant with an average flow rate of 1739.9 Kgpm and a maximum flow rate of 1771.7 Kgpm (15 July). There are a few short duration outages of some pumps which results in a slightly reduced flow rate. The average difference in temperature between the intake and discharge was 17.17 °F and the maximum was 18.8°F, which occurred on 20 July. The discharge temperature (not shown) varied between 94°F and 103°F during this period, which resulted in surface River temperatures measured within the inferred mixing zone at thermistor station 25 reaching 95.1°F. The rejected heat, shown in the lower panel, calculated as the product of discharge flow and discharge temperature rise and converted to appropriate units, shows a near constant amount of heat with few small excursions from the mean. The maximum rejected heat for the period was 4819.9 MWt (30 July), while the average rejected heat from Indian Point was 4383.3 MWt.

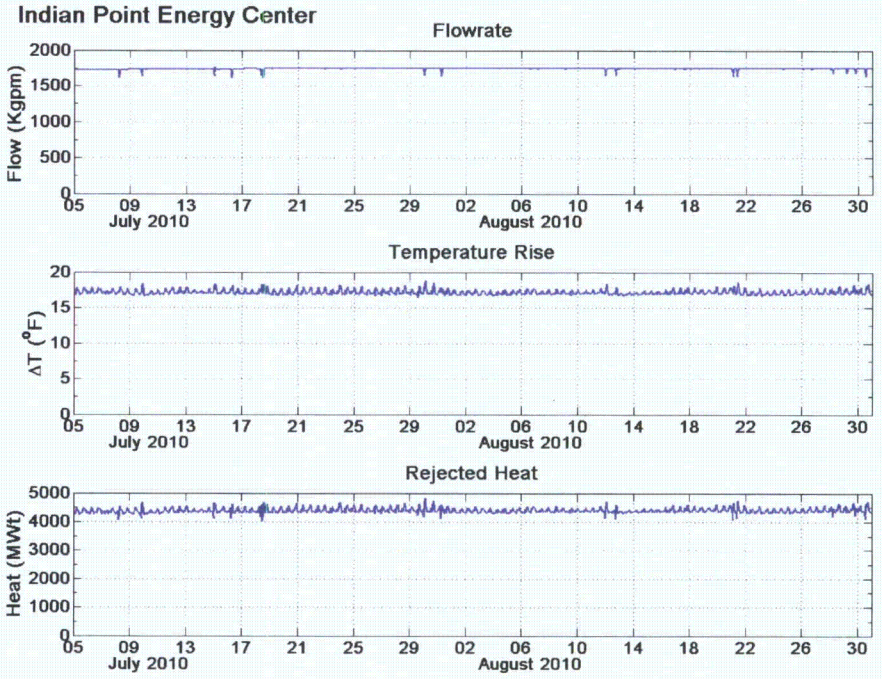

Figure 3-43. IPEC flowrate (upper panel), temperature rise (middle panel) and computed rejected heat (lower panel) during 2010 survey period.

3.7 Other Plant Operations

Three other power plants were in operation in the summer of 2010 along the River as shown in Figure 3-44. The three plants are not in continuous operation but generally operate at discrete times throughout the summer months, including during the 2010 study period. Because they all release thermal effluent into the Hudson River, main periods of operation and heat rejected into the River was addressed.

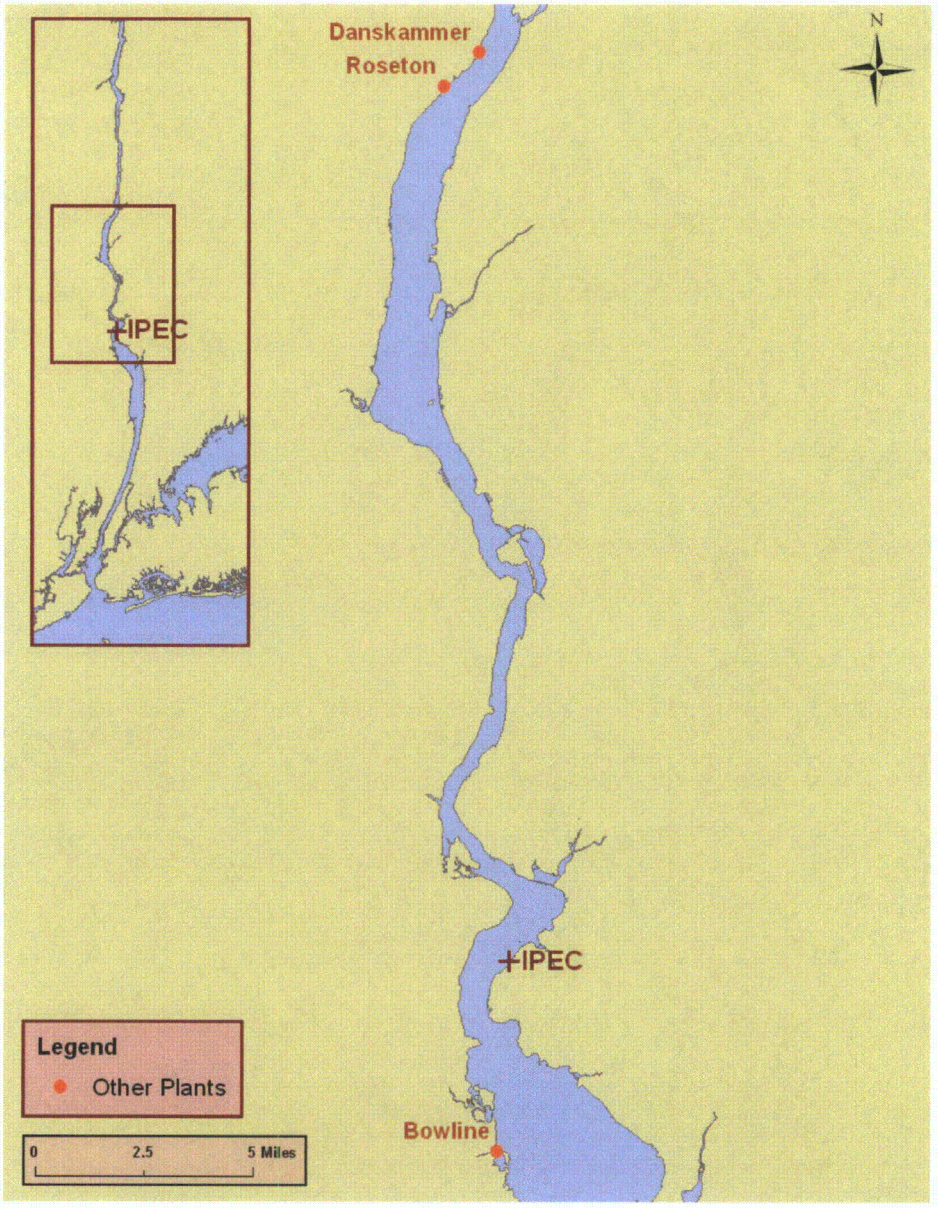

Figure 3-44. Location of IPEC, Danskammer, Roseton, and Bowline power plants along the Hudson River.

The Roseton Units 1 and 2 are located at RM 66 on the western side of the River in the town of Newburgh, NY, approximately 23 miles north of IPEC. The two gas/oil powered steam electric units have

a combined capacity of 1248 MW. Water withdrawn from the River is used to condense steam in the plant and is discharged back into the River as heated effluent (Central Hudson Gas et al., 1999). Daily flow and temperature records for the Roseton and Danskammer Generating Plants were received from Mark Mattson (NAI) for the July through September 2010 period. The rejected heat was calculated based on the flow and temperature differential between the discharge and intake temperatures.

Figure 3-45 displays the flowrate, difference in temperature between intake and discharge, and the calculated rejected heat based on daily operational values. The maximum flowrate at Roseton for the two combined units was 521.7 Kgpm. The maximum difference in temperature due to the cooling process was 10°F, with an average difference of 6.1°F when the plant was in operation. The rejected heat reached as high as 764.6 MWt during the course of the study period, with an average of 390.3 MWt.

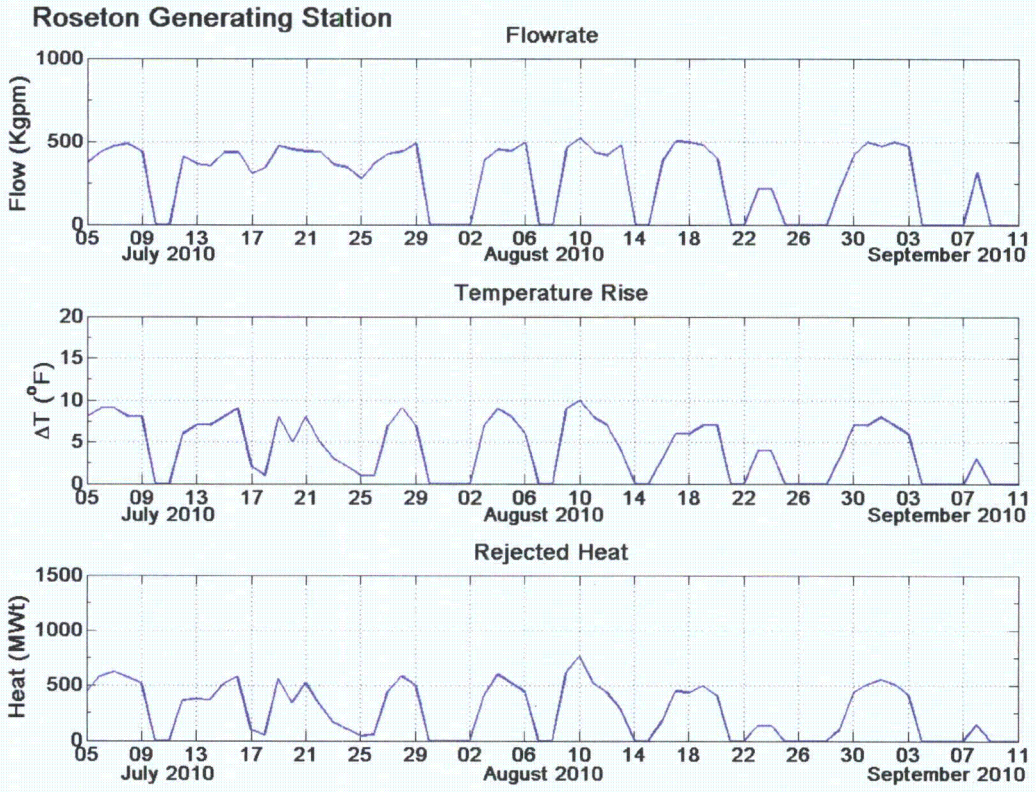

Figure 3-45. Roseton flowrate (upper panel), temperature rise (middle panel) and computed rejected heat (lower panel) during 2010 survey period.

Danskammer, which is located approximately 0.5 mi north of Roseton at RM 66.5, consists of 4 fossil-fuel, steam electric units with a combined capacity of 500 MW. Cooling water for this station is also drawn from the River and returned as heated effluent, with a peak flow of cooling water of approximately 13.2 Kgpm (LMS, 2005).

Figure 3-46 displays the flowrate, difference in temperature between intake and discharge, and the calculated rejected heat based on daily operational values for Danskammer. The maximum flowrate for the four combined units was 281.8 Kgpm. The maximum difference in temperature due to the cooling process was 18°F, with an average difference of 15.2°F when the plant was in operation. The rejected heat reached as high as 616.6 MWt during the course of the study period, with an average of 447.7 MWt.

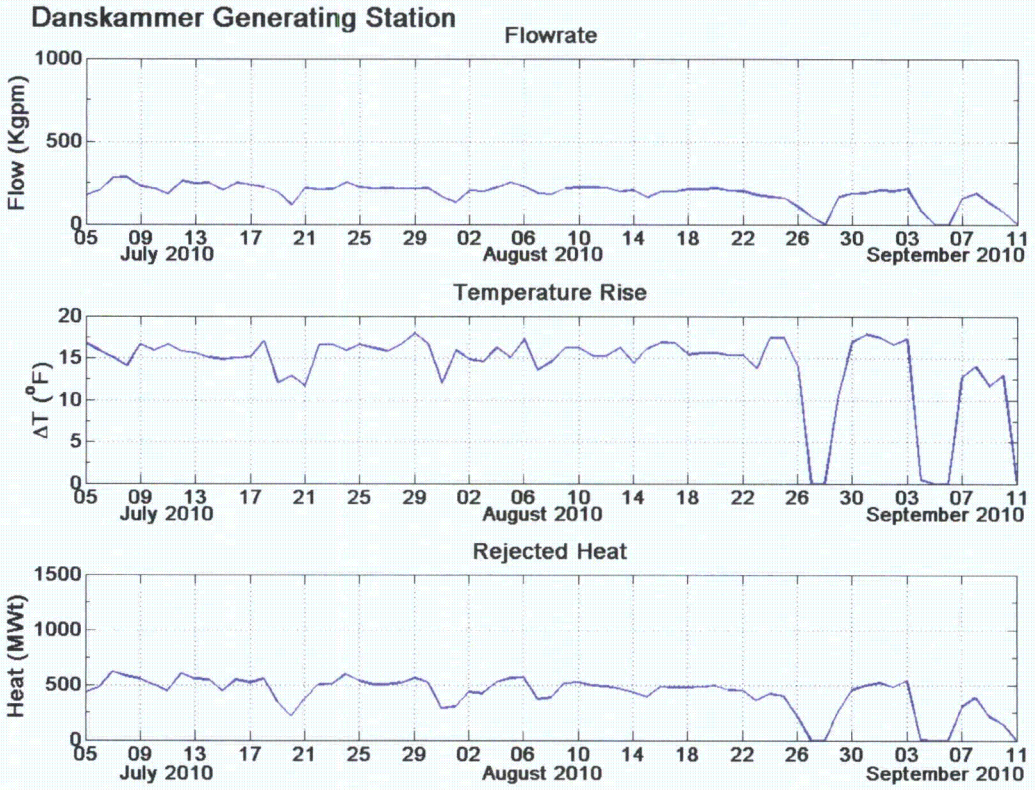

Figure 3-46. Danskammer flowrate (upper panel), temperature rise (middle panel) and computed rejected heat (lower panel) during 2010 survey period.

The Bowline Point generating station is located at RM 37, approximately 6 mi downstream from IPEC, along the western edge of Haverstraw Bay. Bowline is comprised of two gas and oil powered steam electric units. The total combined capacity of the plant is 1200 MWe. The steam units are cooled with a once-through cooling system with water taken from Bowline Pond and discharged into the River 1300 ft from the shoreline (Central Hudson Gas et al., 1999). Daily circulating water use and temperatures were obtained for July, August and September, from which the rejected heat was calculated.

Figure 3-47 displays the flowrate, difference in temperature between intake and discharge, and the calculated rejected heat based off of daily operational values for Bowline. The maximum flowrate for the four combined units was 883.2 Kgpm. The maximum difference in temperature due to the cooling process was 15.5°F, with an average difference of 8.4°F when the plant was in operation. The rejected heat reached as high as 1418.1 MWt during the course of the study period, with an average of 583.7 MWt.

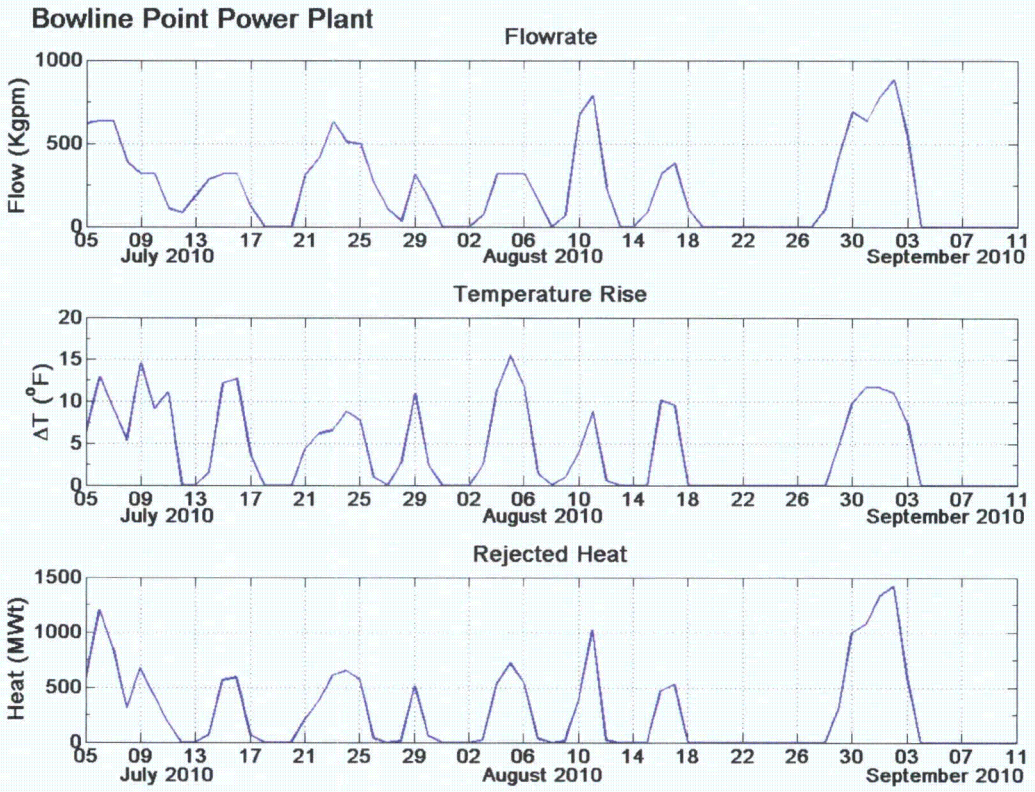

Figure 3-47. Bowline flowrate (upper panel), temperature rise (middle panel) and computed rejected heat (lower panel) during 2010 survey period.

4 Model Application to 2010 Field Data

4.1 Model Forcing For Validation Period

The period chosen for the model validation was a portion of the 2010 time period over which in-River measurements from all instruments (thermistors, ADCPs and public data) and other data were available which spanned the field program dates 5 July though 11 September. The validation period selected was from 8 July through 30 July, which covered a full spring/neap tidal cycle and included the warmest in-River temperatures as well as a range of temperatures, captured in the warming trend early in the period. The environmental conditions during this period approached the extreme environmental conditions occurring during August 2005 identified in Swanson et. al. (2010b) and so was a good period in which to determine IPEC compliance with Thermal WQS. The model was driven at its open boundaries, which included the lower River boundary at Hastings on Hudson, the upper River boundary at Green Island, the water-air boundary at the River surface, and the plant thermal discharges along the River. Figure 4-1 shows the River from Hastings-on Hudson to Troy, along with USGS stations at Hastings on Hudson, West Point, Poughkeepsie, Albany, and Green Island; the Danskammer, Roseton, Indian Point and Bowline power plants; and the White Plains Airport. The data used to drive the model at each boundary is described in the following sections.

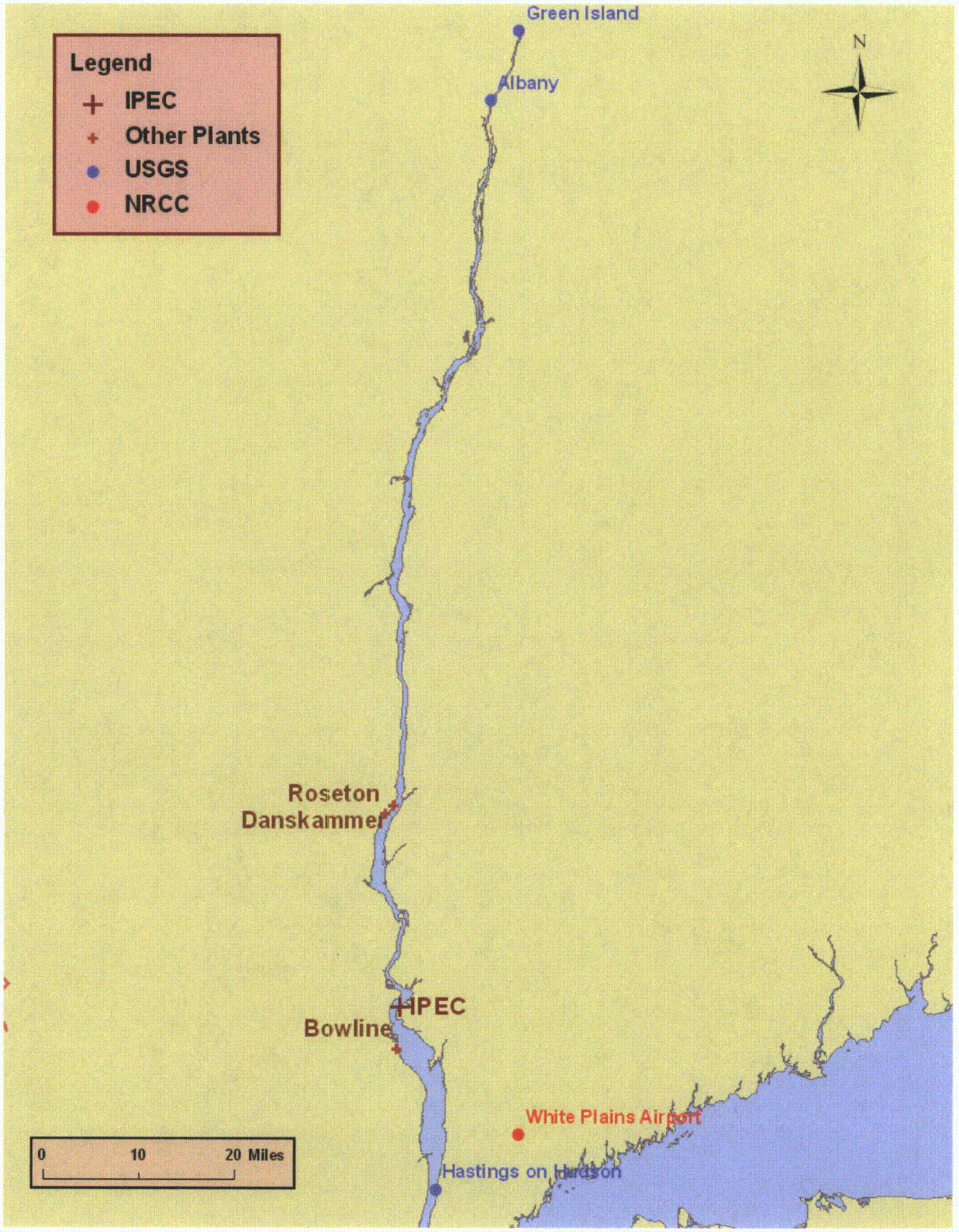

Figure 4-1. Hudson River locations of model input data sources.

4.1.1 River Boundaries

4.1.1.1 Downstream River Boundary At Hastings-On-Hudson

The downstream open boundary forcing used available USGS collected data at Hastings-on-Hudson. The site, designated as 01376304, measured water level, as well as temperature and conductivity at a depth of 10 ft at 15 minute intervals. The conductivity was converted to salinity using the relationship developed empirically by NAI (Texas Instruments, 1976). While other model forcing factors were applied at one hour time steps the lower river boundary forcings were applied at a 15 minute time step; given that surface elevation can change relatively significantly within an hour this method ensures that the minimum and maximum surface elevations are more accurately represented. Figure 4-2 shows the time history over the validation period of water level, temperature and salinity at the lower River boundary at Hastings-on Hudson. The elevation or water level clearly indicates tidal influence at this location in the River. The tide oscillates with a 12.42 period (M2 tidal constituent) and the tidal range changes over the 14.5-day spring-neap cycle. Note that the large gap in the salinity data at Hastings exists for 5 days in the model period as a result of sensor failure as reported by USGS. During that period the salinity was held constant at 9.6 psu for lack of better information.

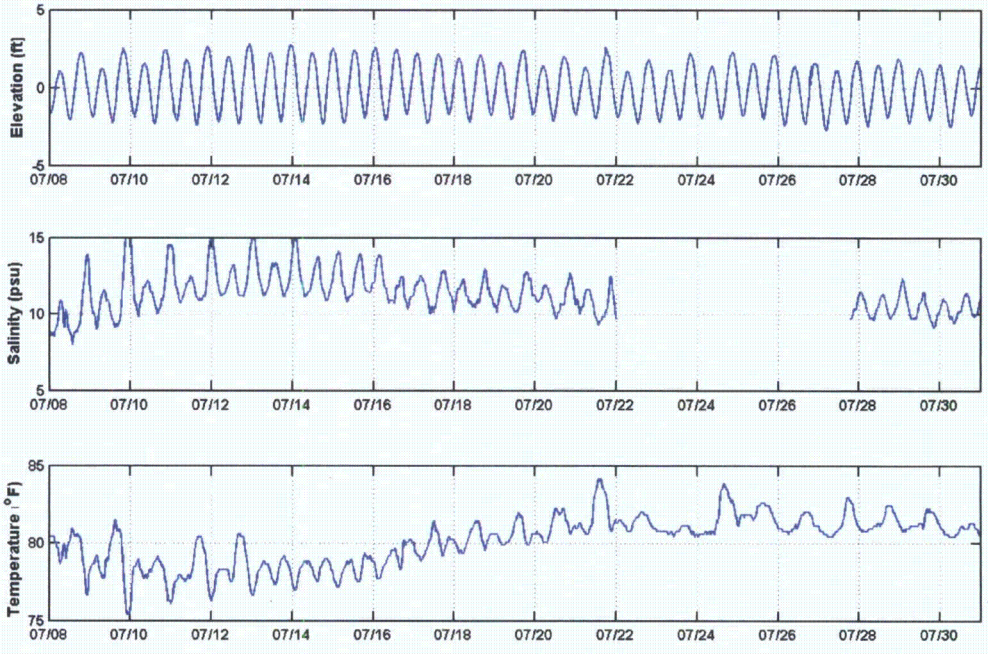

Figure 4-2. USGS water level (upper panel), salinity (middle panel) and temperature (lower panel) measured at Hastings for 8 to 31 July.

4.1.1.2 Upstream River Boundary At Troy

The upstream open boundary forcing used available USGS collected data at two adjacent sites near the dam in Troy. The Green Island site, designated as 01358000, provided River flow rate data, while Albany, designated as 01359139, provided water temperature (salinity was zero), both at 10-ft depths below the surface. A regression between Green Island and Esopus Creek (01362500) was developed to fill data gaps in the Green Island data. Data was provided at 15-min intervals and was processed to

hourly averages and sub-sampled to the hour. Figure 4-3 shows the time history over the validation period for flow rate and temperature.

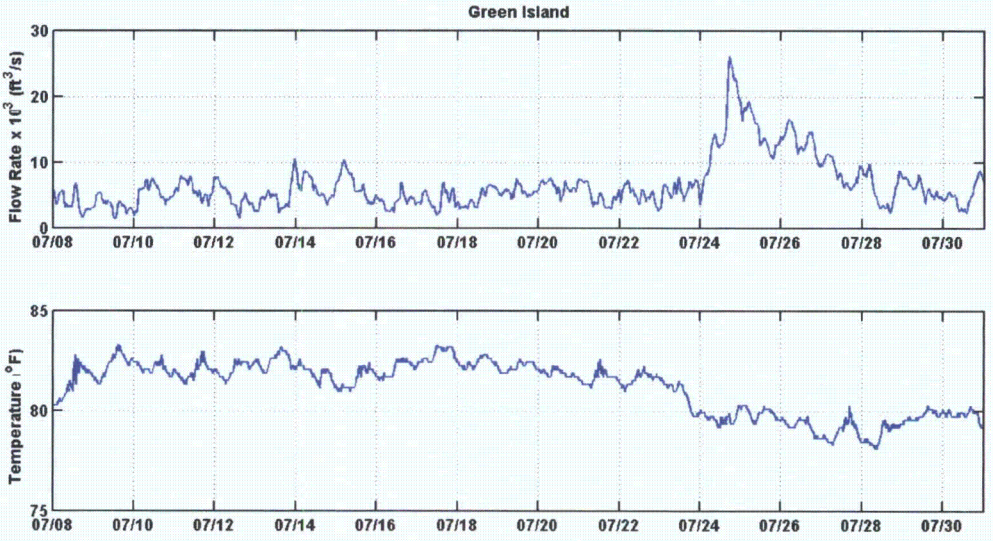

Figure 4-3. USGS flowrate (upper panel) and temperature (lower panel) measured at Green Island for 8 to 31 July 2010.

4.1.2 Meteorological Conditions

The meteorological variables used in the model were those from the White Plains Airport (HPN). The data consisted of air temperature, dew point temperature, relative humidity, wind speed and direction, atmospheric pressure and solar radiation. Figure 4-4 shows the time history of these variables during the validation period. The wind is shown as a vector with its length scaled to the speed and its direction pointing downwind (oceanographic convention).

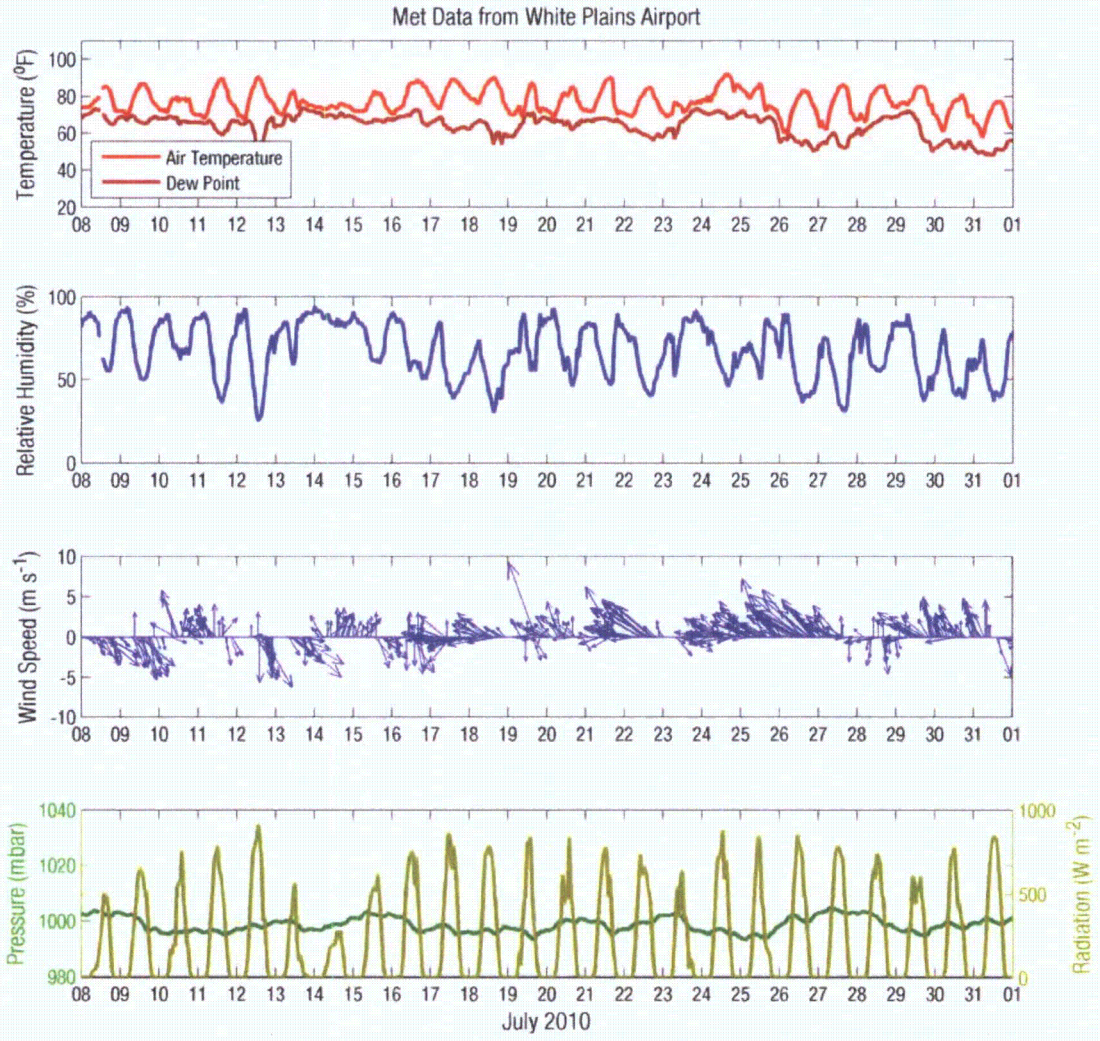

Figure 4-4. NRCC meteorological data measured at White Plains for 8 to 31 July 2010 measured at White Plains.

4.1.3 Plant Thermal Discharges

4.1.3.1 IPEC Operations

Flow and temperature records were provided by IPEC describing their operations during the validation period. Figure 4-5 shows the time history of cooling water flow, intake and discharge temperature, and the calculated rejected heat. The rejected heat calculation was based on the temperature difference between discharge and intake temperatures and the cooling water flow.

IPEC operated at a relatively consistent flow of approximately 1700 Kgpm from 8 July through 30 July, with a few small decreases in flow during pump outages. The temperature rise between intake and discharge varied between 16.5°F and 18.8°F, with an average of 17.2°F. This resulted in a range of rejected heat between 4040 MWt and 4820 MWt, with an average of 4380MWt,

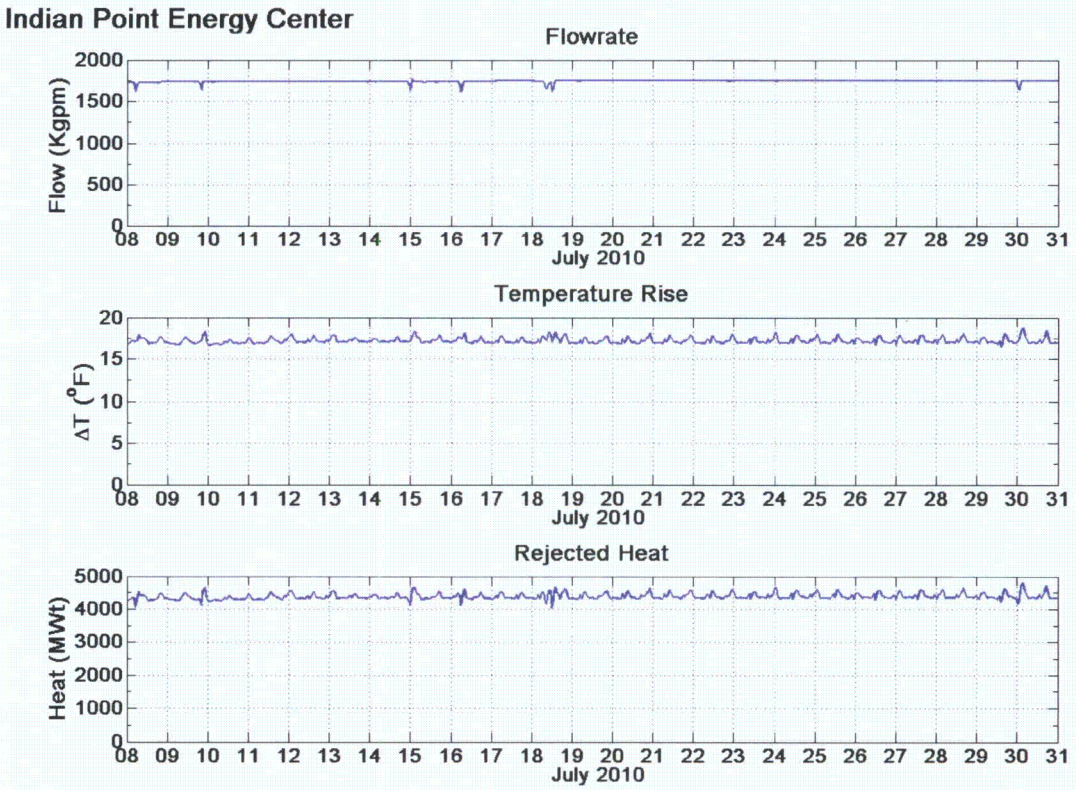

Figure 4-5. IPEC operations (discharge flow [upper panel] and temperatures [middle panel]) with computed rejected heat (lower panel) for 8 to 31 July 2010.

4.1.3.2 Other Plant Operations

Daily flow and temperature records for the Danskammer, Roseton and Bowline power plants were provided by Mark Mattson (NAI) as part of their Daily Operating Reports for the July through September 2010 period. Figure 4-6, Figure 4-7, and Figure 4-8 show the time history of cooling water flow, intake and discharge temperature and the calculated rejected heat for the Danskammer Roseton, and Bowline plants for the validation period, respectively. The rejected heat calculation was based on the flow and temperature difference between discharge temperature and intake temperature.

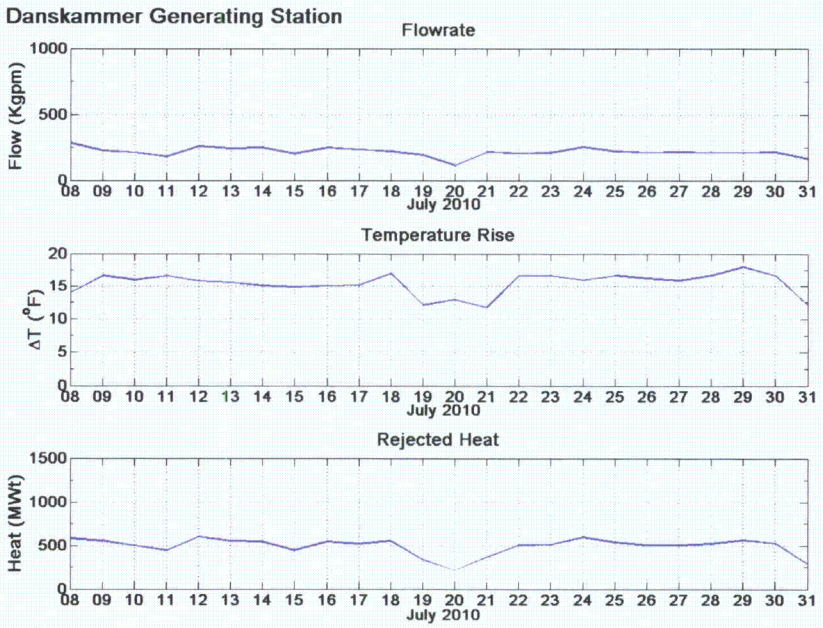

Figure 4-6. Danskammer operations (discharge flow and temperatures) with computed rejected heat for 8 to 31 July 2010.

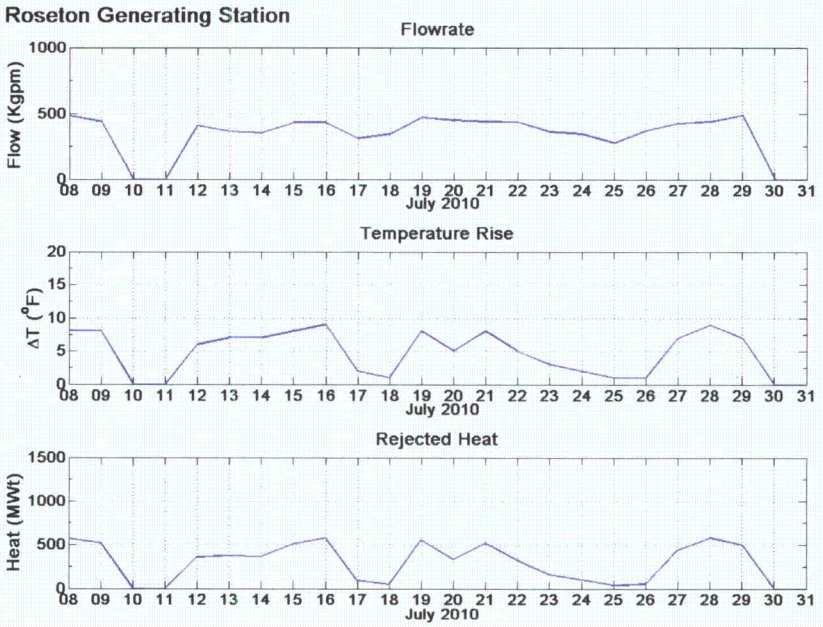

Figure 4-7. Roseton operations (discharge flow and temperatures) with computed rejected heat for 8 to 31 July 2010.

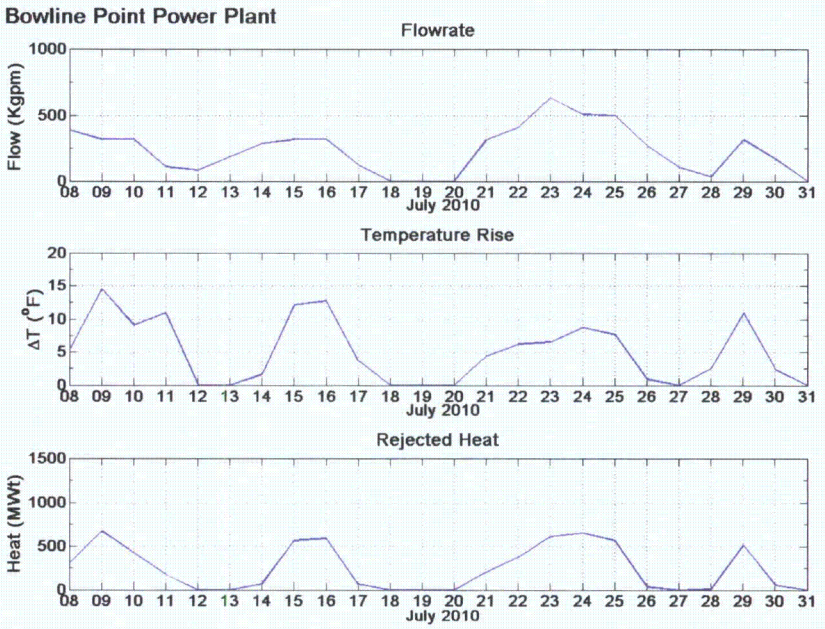

Figure 4-8. Bowline operations discharge flow and temperatures) with computed rejected heat for 8 to 30 July 2010.

4.2 Model Results For 8 through 30 July 2010 Period

The primary focus of the 2010 modeling was to use the previously calibrated model (Swanson et al., 2010b) to simulate the 8 through 31 July 2010 validation period to determine compliance with NYSDEC Thermal WQS. The sections below show comparisons to water level (surface elevation) from USGS stations and ADCPs from the field program, current velocities from the ADCPs and temperatures from selected thermistors deployed as part of the field program as well as USGS stations.

The model system was set up and run identically for the validation simulations as it was for the calibrations simulations to the 2009 field data. Therefore all of the model parameters used to calibrate the earlier application (Swanson et al., 2010b) were used in these simulations as well.

The model grid domain was initialized using an average temperature equivalent to the average of the recorded values at Hastings and West Point, at the south and north ends of the IPEC study area. The salinity was initialized with a linear gradient from 1 psu at IPEC to an average of 12 psu at Hastings at the open boundary at the southern extreme of the model grid. The model simulations were initialized to begin on 1 July 2010 and ran for a 7-day period to allow the model to equilibrate initial and boundary conditions to the internal distribution of water surface elevation, currents, temperature and salinity. The validation period simulations then began on 8 July 2010 and ran through 30 July 2010 driven only by the external forcing of the tides, rivers, plant flows and temperatures and atmospheric conditions.

The surface elevation variation at the open boundary at Hastings drives the tidal response in the River domain, seen as tidal currents moving upstream on the flood tide and downstream on the ebb tide. These tidally driven currents in the IPEC area and elsewhere are the primary force moving the IPEC thermal plume in the River. An example of the tidal dynamics of the model predicted currents and the response of the thermal plume is presented in Figure 4-9 showing eight stages through the tidal cycle. The area in the figures extends from south of Stony Point to just north of Peekskill Bay.

The series begins at slack tide before ebb (Figure 4-9 a), when the currents in the area are relatively small and the thermal plume begins to pool in the area of the IPEC discharge, where the model predicted surface temperatures are presented as color coded contours. This condition persists for only a short time, and the tidal currents begin to ebb such that an hour later (1 hr after slack before ebb) the pooled plume has moved and stretched in the downstream direction (Figure 4-9 b).

The current vectors can also be seen on the plot, pointing along the river in a downstream direction. The number of vectors has been reduced so that only every fourth vector is shown in both the along-channel and across-channel directions, for the sake of clarity. The size of the vector is an indication of the current speed at that location in the River. There is a variation in the current speeds across the River where currents tend to be larger in the center of the River along the channel with the majority of the flow, and slower along the shorelines where the water is shallower and there is higher friction retarding the flow.

In addition, a vertical section taken across the river at the IPEC outfall is shown on the right side of each plot. The thermal plume appears in the upper right of each of the vertical sections indicating the cross channel and vertical extent of the plume for each tidal stage. Finally, there is an environmental time series of solar radiation and tidal elevation at Hastings presented in the lower right of each panel. A vertical line on the time series indicates the appropriate time for the time of the picture.

As the tidal velocities approach maximum ebb values, the thermal plume is further stretched along the River and diluted by the entrainment of the tidal currents passing the plant, appearing as a decrease in temperatures that can be seen in the color coded temperature contours in Figure 4-9 c and d. The plume is primarily transported downstream along the east side of the river carried by the strong along-channel currents, preventing it from extending across the River.

The river currents slow as the tidal stage approaches slack before flood at which time the thermal plume has essentially dispersed downstream and begins to pool again at the outfall area, shown in Figure 4-9 e and f. The tidal currents then rise, driving the flood tidal currents in up-River, also moving the plume in that direction (Figure 4-9 g and h), although not as far downstream during ebb. This is primarily due to the fact that there is a net downstream flow at the surface, associated with the river flow and gravitational circulation, meaning that the surface currents are larger in the downstream direction than in the upstream direction.

An important aspect of the temperature dynamics in the River can also be seen in the plots presented in Figure 4-9. Figure 4-9 g and h, which simulate the afternoon, show that the model predicts some diurnal (daily) heating of the surface waters in the shallow area in Green's Cove on the east side of the River across from Stony Point. This can be seen as a light green color temperature contour in Green's Cove. The diurnal heating is due to both solar radiation and air temperatures heating the entire water body but affecting the shallower areas along the edges of the River to a greater extent. This is also therefore a separate and distinct localized heat source to the River.

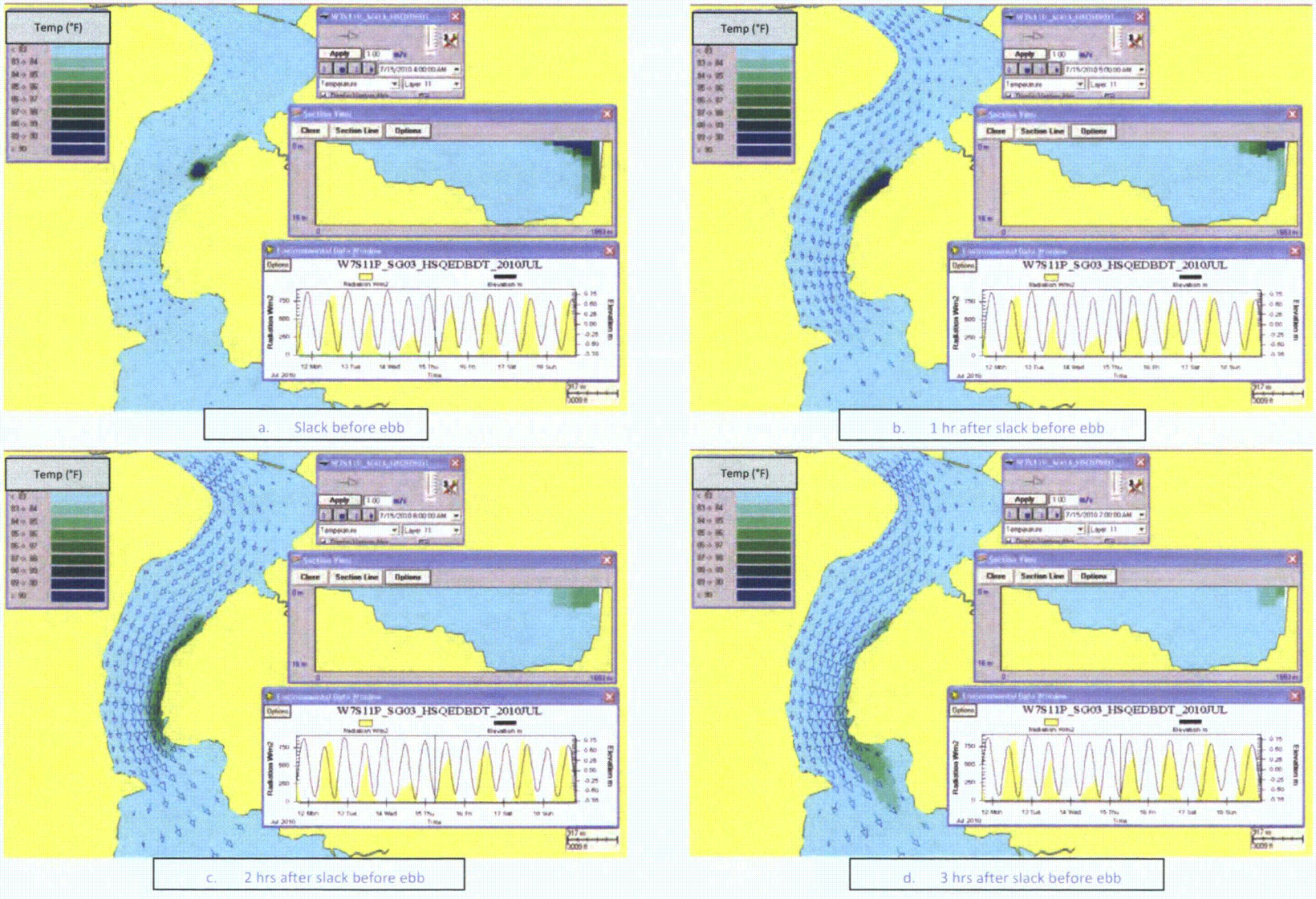

Figure 4-9. Panels a-d. Plan view of the model predicted surface temperatures showing the maximum downstream extent of the plume near slack before ebb during the period from 8 July through 30 July 2010.

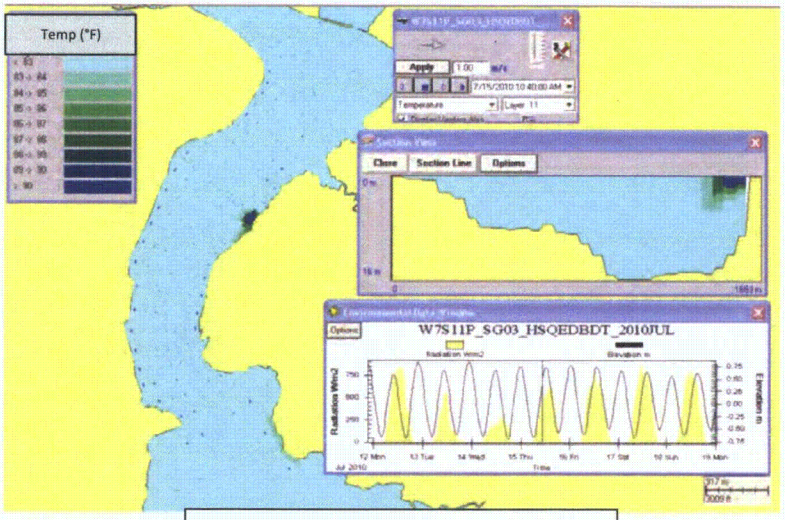

e. 1 hr before slack before flood

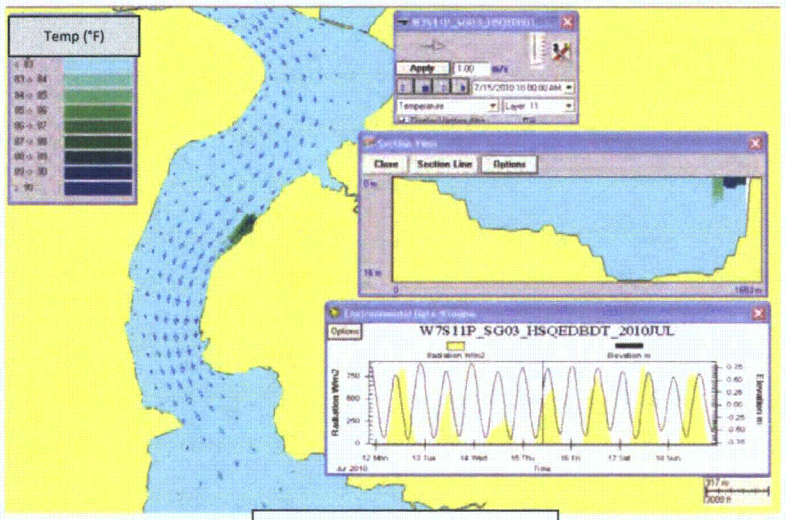

f. Slack before flood

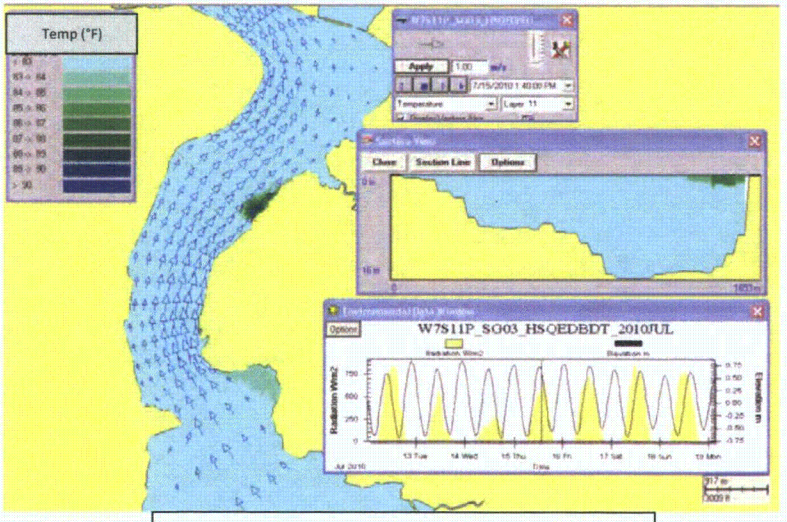

g. 3 hrs after slack before flood (max flood)

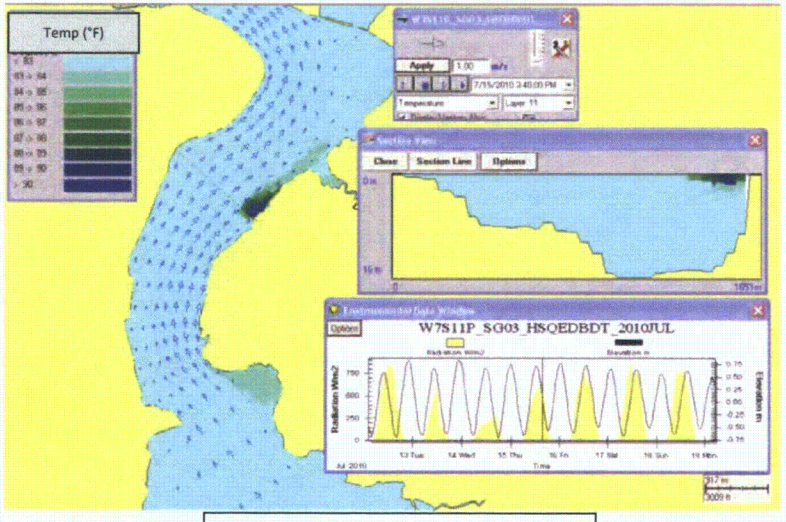

h. 1 hr before slack before ebb

Figure 4-9. Panels e-h. Plan view of the model predicted surface temperatures showing the maximum downstream extent of the plume near slack before ebb during the period from 8 July through 30 July 2010.

An example of the maximum extent of the plume is presented for the downstream direction in Figure 4-10 and the upstream direction in Figure 4-11. The River area depicted in the figures extends from Peekskill Bay in the north down to Croton Point in the south, including Haverstraw Bay. These figures show the model-predicted water surface temperatures for a representative slack before flood tide and slack before ebb tide, respectively, from the validation time period. The majority of the transport of heated discharge is along the eastern side of the River, decreasing in temperature with distance across the channel as well as along the channel. There is also a bias to the south with the net downstream transport at the surface associated with the river flow. The thermal discharge from the Bowline plant can be seen on the west side of the River between Croton and Stony Points during this time period. The diurnal, (solar and air temperature) heating to the shallows in Haverstraw Bay is also clearly visible in Figure 4-10, particularly on the east side of the River just north of Croton Point.

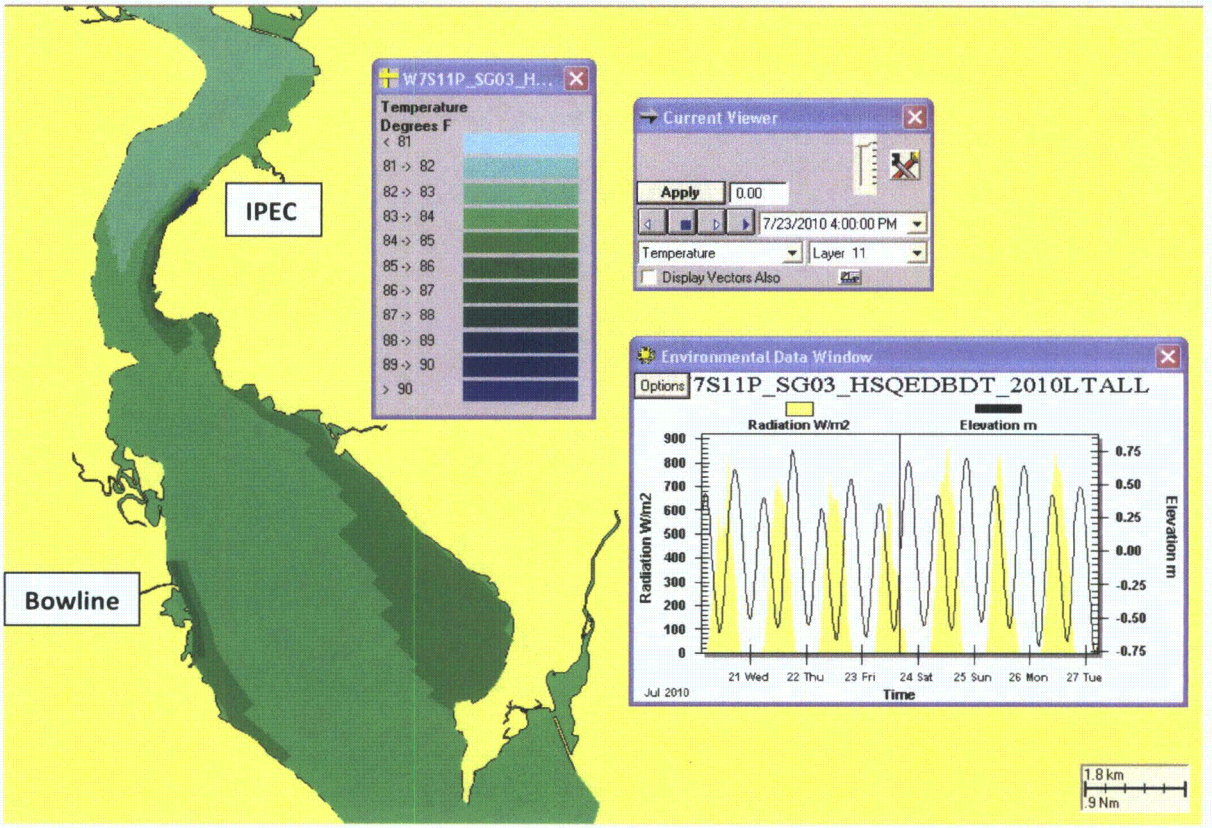

Figure 4-10. Example plan view of the model predicted surface temperatures showing the maximum downstream extent of the plume near slack before flood.

In Figure 4-11 depicting the slack before ebb conditions, the thermal plume from the Bowline plant is again visible, heading north along the west side of the River. The extent of the Bowline thermal plume does not appear large at any time and, as it moves in the same direction as the IPEC thermal plume responding to the tidal currents, and is on the opposite side of the River, it does not interact with the IPEC thermal plume.

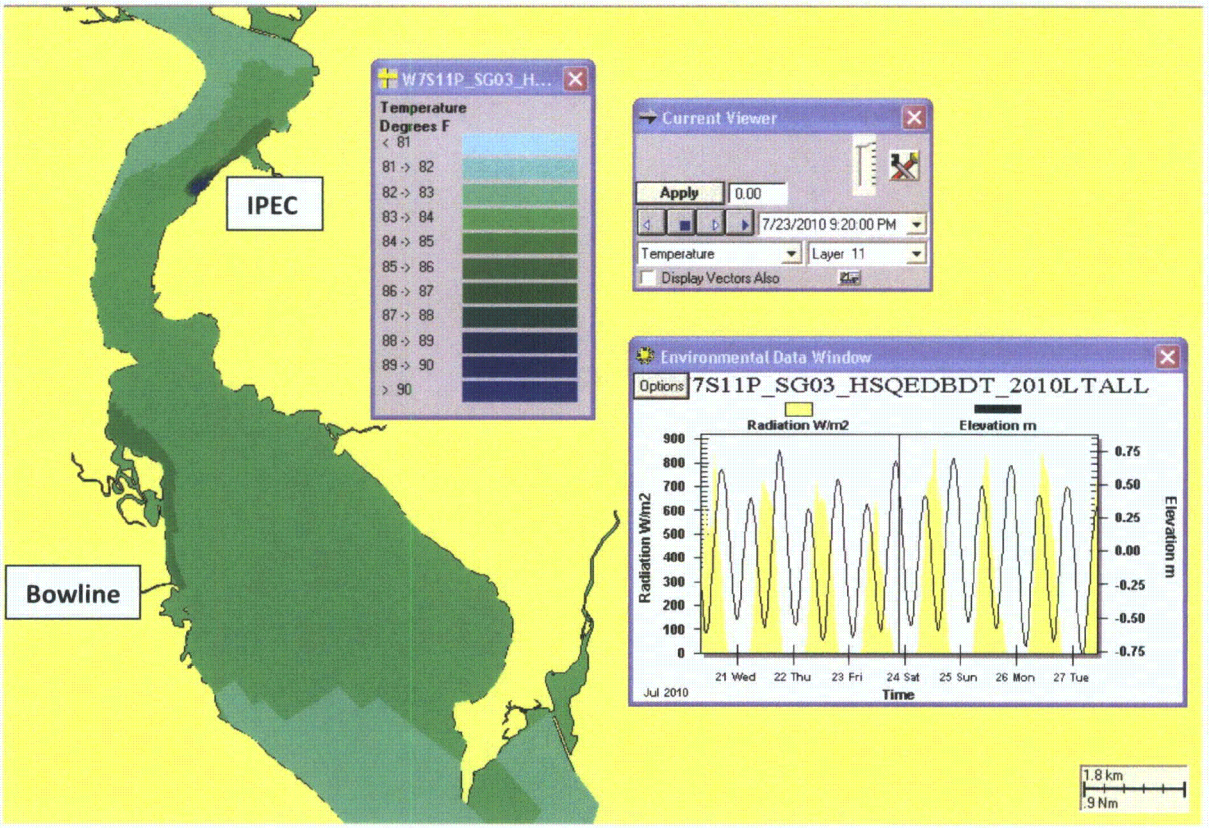

Figure 4-11. Plan view of the model predicted surface temperatures showing the maximum upstream extent of the plume near slack before ebb.

The forgoing discussion provides an overview and qualitative description of the tidal circulation and temperature dynamics in the River. In addition to capturing and understanding the plume dynamics and its spatial extent, it is of interest to compare the model predictions during the validation time period in a quantitative manner to observations at particular points along the River where data was taken during the summer 2010 field program. The following sections compare the model predictions to observations for water surface elevation, current, and temperature time series at various locations in the River.

4.2.1 Procedure for Comparison of Model Predictions to Observations

4.2.1.1 Qualitative Comparisons

The comparison of model results and observations depends on data dimensionality. For example, a time series of data collected at a particular site can be plotted together with model output to provide a visual comparison. This comparison can provide information on the suitability of the model to simulate the range of variability evident in the observations.

The most direct way to provide a qualitative comparison is to plot the model predictions and the observed data for each variable over the time of the simulation. This can be done with time series plots of the variables of interest or contour plots when looking at spatially varying patterns.

4.2.1.2 Quantitative Comparisons

Quantitative comparisons are statistical measures that can be applied to the model predictions and field data sets that provide a numerical assessment of the comparison. These statistical measures can be grouped into two major components: those measures that describe an individual set of data (e.g., a time series of one variable), and those that relate the degree of difference (error) between two data sets (e.g. time series of model predictions and field observations). Individual statistical measures include the mean, standard deviation, percentiles, minimum, and maximum. The independent variable can be time, depth or distance in these data. The quantitative comparisons between data sets include relative error, root mean square error, linear regression, comparison of means and correlation coefficient.

For the present study a combination of statistics was used to assess the model validation in a method identical to the calibration study. The statistical measures used were the correlation coefficient, r^2, relative error of the means, (RME), error coefficient of variation (ECV) and the model "skill". McCutcheon et al (1990) describes these quantitative comparisons in detail, and provides guidance on acceptable values with the exception of skill, which is described in Warner et al (2005). Each of the statistical measure used in this analysis are described in detail in Swanson et al (2010b).

4.2.2 Water Level

Water surface elevation is the primary driver of circulation in the system. The currents are generated as a result of the tidal oscillations at the southern boundary of the River, represented at Hastings for this model application. The observations used for comparison to the model predictions are time series of water level (surface elevation) from the USGS stations at West Point, Poughkeepsie, and Albany and from the ADCPs at Stony Point, Indian Point and Iona Island deployed as part of the field program.

A comparison of the model predicted time series at the three upstream USGS stations is presented in Figure 4-12. The figure shows the model predictions in blue and the observations in red. The model clearly simulated the tide range and phase well, which varied considerably throughout the system, increasing in amplitude to a maximum seen at Albany. While the upstream stations are of interest, and necessary to provide the flow dynamics to the area closer to IPEC, the comparison to the stations in the Indian Point area are of greater interest. Figure 4-13 shows the comparison of model-predicted elevations to observations at the three ADCP locations at Stony Point, Indian Point and Iona Island. An excellent fit was found at all three locations, where the time series essentially overlaid one another, meaning that the model sufficiently captured the tidal dynamics in this important portion of the River.

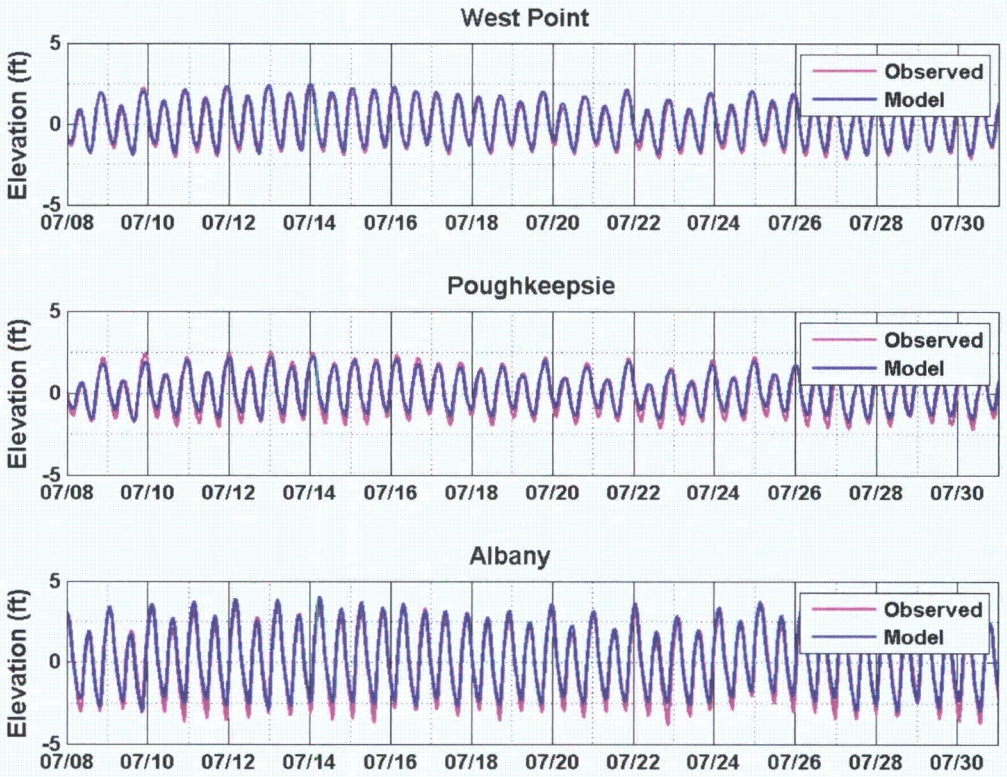

Figure 4-12. Water level comparison between model predictions and observations for the validation period from 8 through 30 July 2010 for West Point (upper panel) , Poughkeepsie (middle panel) and Albany (lower panel).

Table 4-1 summarizes the set of quantitative statistical measures for the USGS stations with surface elevation observations. For surface elevation statistical calculations of RME and ECV the mean was assumed equal to the tidal range to make them a useful measure of variance, otherwise the mean would be approximately zero as tide ranges oscillate close to zero relative to man sea level.

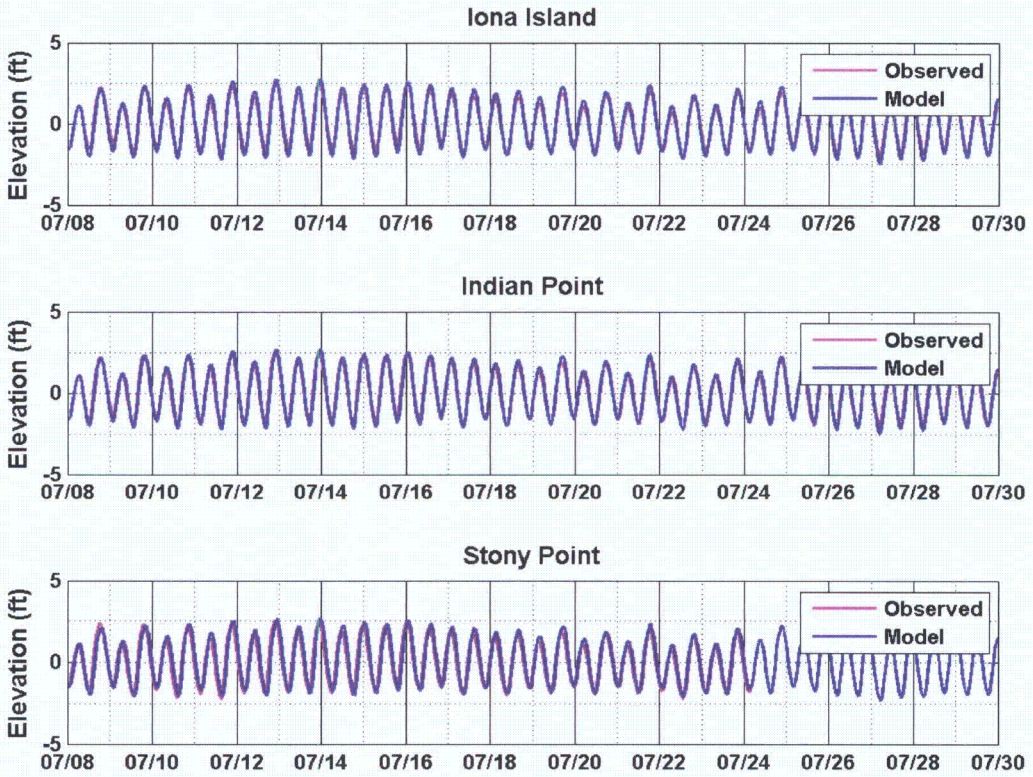

Figure 4-13. Water level comparison between model predictions and observations for the validation period from 8 through 30 July 2010 for ADCPs deployed at Iona Island (upper panel), Indian Point (middle panel) and Stony Point (lower panel).

Table 4-1. Quantitative comparisons of predicted and observed tidal range at USGS and ADCP locations during the period from 8 to 31 July 2010.

Station	r^2	RME	ECV	Skill
West Point	0.98	-2.7%	0.1%	0.99
Poughkeepsie	0.98	-2.7%	0.1%	0.98
Albany	0.99	-3.0%	0.1%	0.99
Stony Point	0.92	-0.2%	0.3%	0.98
Indian Point	0.98	-0.2%	0.2%	0.99
Iona Island	0.96	0.0%	0.1%	0.99
Average	**0.97**	**1.5%**	**0.2%**	**0.99**
Guidance	**0.94**	**±30%**	**10%**	**0.90**

An additional assessment of the tidal elevation can be found in the comparison of the tidal harmonic constituents. For this analysis, the tidal elevation oscillation was analyzed and broken down into its constituent harmonic frequencies at well known frequencies or periods. For example the largest tidal

constituent is the M2 with a 12.42 hr period, resulting in the twice daily rise and fall of the tides. The most important constituents in this portion of the River (based on relative size) are the M2, K1 and O1 components, which together create the higher high tides and lower low tides in the area. The constituent components were compared at each of the USGS and ADCP locations and are presented as a function of river mile as shown in Figure 4-14. Similarly, the phase of each component, which is the relative timing of its peak, is presented as a function of river mile in Figure 4-15.

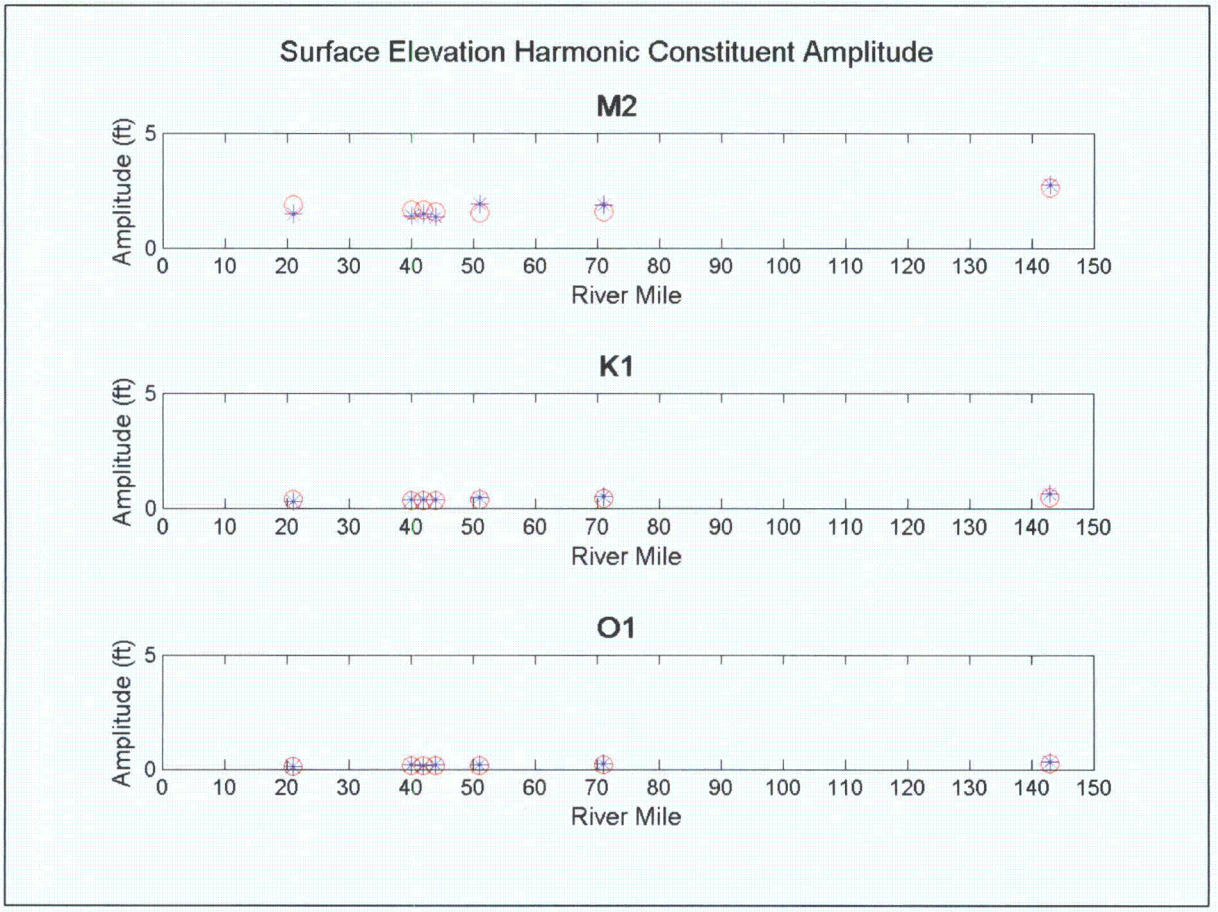

Figure 4-14. Water surface elevation harmonic constituent amplitude comparison between model predictions and observations for the validation period from 8 through 30 July 2010 for the M2 (upper panel), K1 (middle panel) and O1 (lower panel) components.

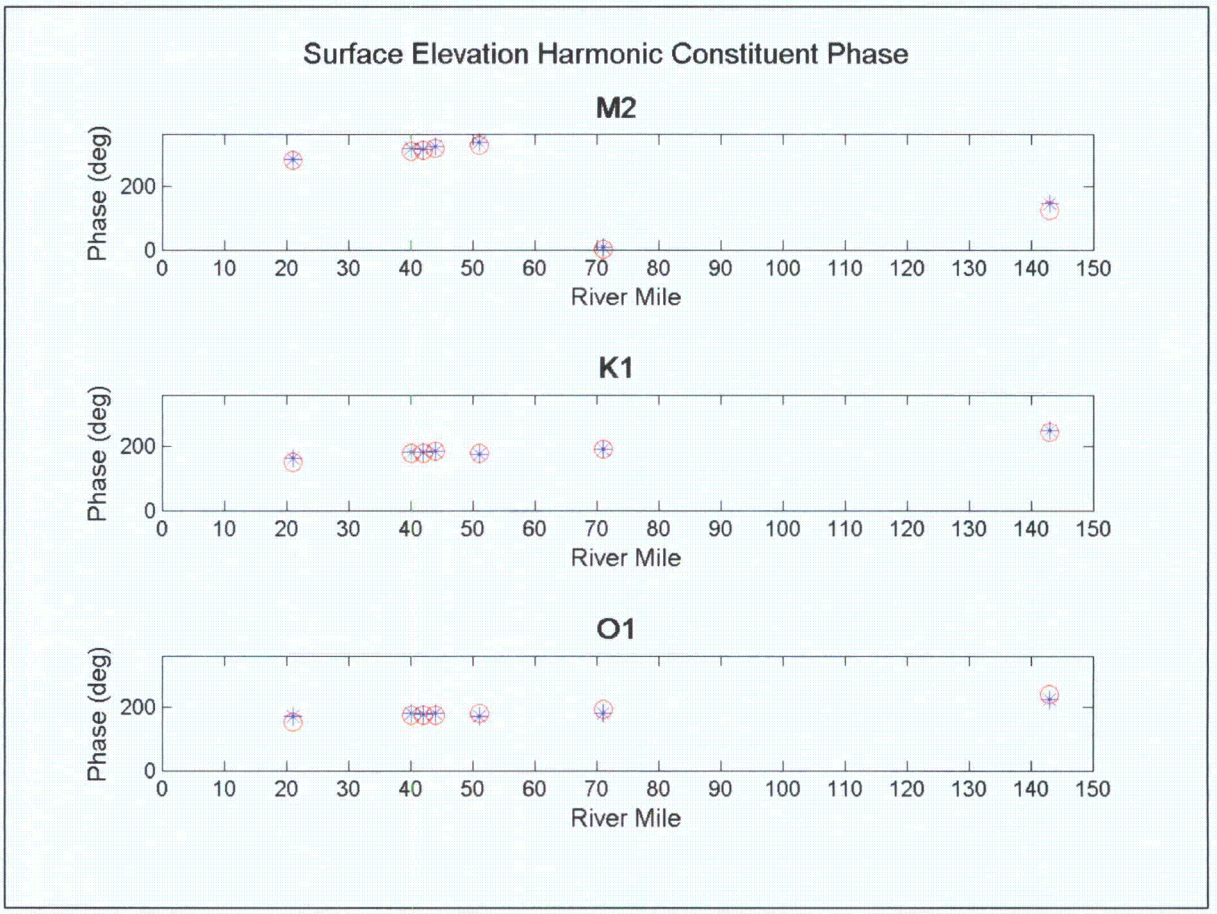

Figure 4-15. Water surface elevation harmonic constituent phase comparison between model predictions and observations for the validation period from 8 through 30 July 2010 for the M2 (upper panel), K1 (middle panel) and O1 (lower panel) components.

Table 4-2 summarizes the quantitative comparison of statistics for the harmonic constituent analysis at each of the stations. The results show that the model performed well at all locations, capturing the 180 degree phase shift in tidal elevation (i.e., when the tide is low at Hastings, it is high at Albany) along the 150 mile-long River. In addition, the model tracked the observed trend of increased tidal amplitude in the northern portion of the River well, increasing from West Point to Albany by over 1 ft.

Table 4-2. Quantitative comparisons of summary statistics for the harmonic constituent analysis at the USGS and ADCP locations during the period from 8 July 2010 to 31 July 2010.

Harmonic Constituent	Station	Observed Amplitude (ft)	Model Amplitude (ft)	Difference (ft)	Observed Phase (deg)	Model Phase (deg)	Difference (deg)
M2	West Point	1.57	1.95	0.38	328	336	8
	Poughkeepsie	1.6	1.92	0.32	2	7	5
	Albany	2.63	2.77	0.14	124	146	22
	Stony Pt	1.69	1.44	-0.25	310	319	9

Harmonic Constituent	Station	Observed Amplitude (ft)	Model Amplitude (ft)	Difference (ft)	Observed Phase (deg)	Model Phase (deg)	Difference (deg)
	Indian Pt	1.7	1.5	-0.20	313	315	2
	Iona Is	1.59	1.38	-0.21	319	325	6
K1	West Point	0.36	0.44	0.08	179	175	-4
	Poughkeepsie	0.4	0.48	0.08	190	188	-2
	Albany	0.45	0.63	0.18	246	250	4
	Stony Pt	0.34	0.36	0.02	176	181	5
	Indian Pt	0.33	0.36	0.03	179	179	0
	Iona Is	0.34	0.37	0.03	182	184	2
O1	West Point	0.16	0.21	0.05	179	169	-10
	Poughkeepsie	0.19	0.24	0.05	189	178	-11
	Albany	0.23	0.32	0.09	236	222	-14
	Stony Pt	0.14	0.18	0.04	170	178	8
	Indian Pt	0.16	0.18	0.02	172	176	4
	Iona Is	0.16	0.19	0.03	173	180	7

4.2.3 CURRENTS

Three ADCPs were deployed during the field program, one to the north of Indian Point near Iona Island (II) a second near IPEC (IP) and a third at Stony Point (SP) south of Indian Point. The current velocities recorded from the ADCPs were rotated to along-River direction to more clearly show that most of the flow travels in the up and downstream directions. The II ADCP data were rotated, 45 degrees west of north, IP data were rotated 50 degrees east of north and the SP data were rotated 50 degrees west of north.

Figure 4-16, Figure 4-17, and Figure 4-18 show the time series of current velocities at the surface and bottom layers, respectively, at Iona Island, Indian Point, and Stony Point. The surface currents in all three locations show the strong tidal variation moving up and down with the period of 12.42 hours. In addition, the simulated results captured bi-weekly spring-neap tide as well as diurnal inequality in successful manner. The simulated flow is slightly larger than the observations. The bottom currents while tending to be over predicted when compared to observed again show the strong tidal variation moving up and down river. The simulations capture the reduced bottom currents compared to the higher surface currents.

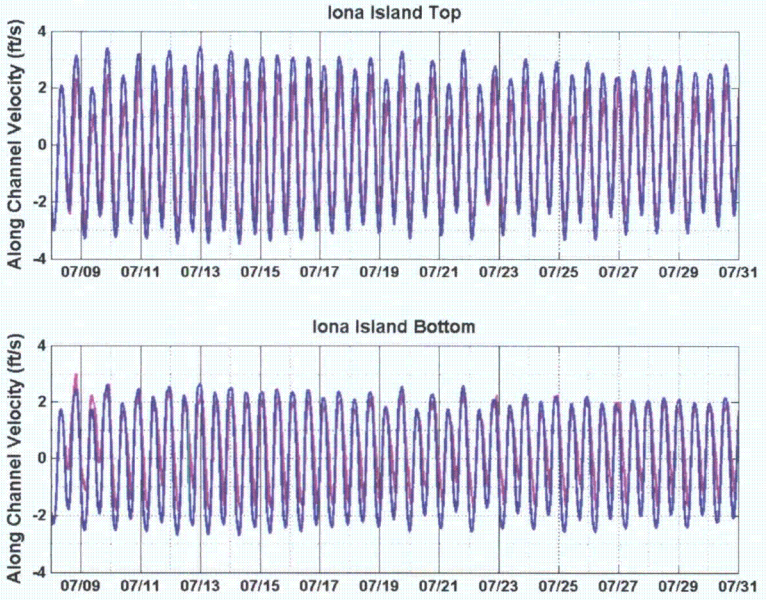

Figure 4-16. Near surface (upper panel) and near bottom (lower panel) along channel current comparison between model predictions and observations for the period from 8 through 30 July 2010 at Iona Island.

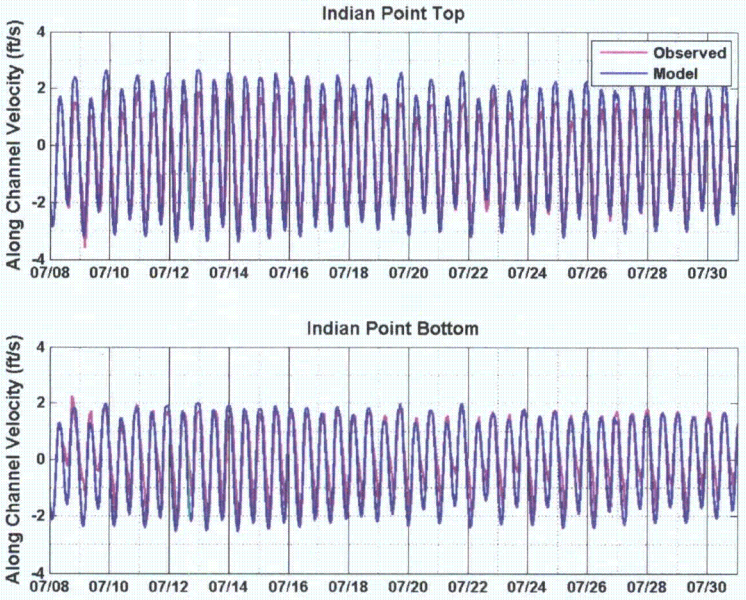

Figure 4-17. Near surface (upper panel) and near bottom (lower panel) along channel current comparison between model predictions and observations for the period from 8 through 30 July 2010 at Indian Point.

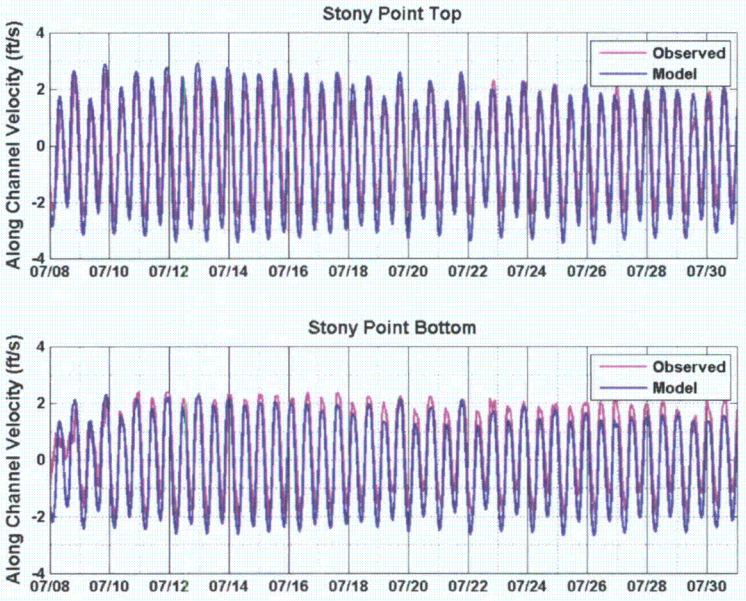

Figure 4-18. Near surface (upper panel) and near bottom (lower panel) along channel current comparison between model predictions and observations for the period from 8 through 30 July 2010 at Stony Point.

The quantitative statistical measures for the currents from the three ADCPs are presented in Table 4-3. In accordance with the time-series data presented above, the average statistics in this summary table shows that the current patterns were successfully simulated by the model in that the model results were within the guidance values for RME, ECV and Skill but was slightly below for r^2. The results show that the model predictions were moderately better for surface currents than the bottom currents, which is relevant since most of the thermal plume transport is within the surface layer of the water column.

Table 4-3 Quantitative comparisons of predicted and observed surface and bottom currents at Iona Island, Indian Point, and Stony Point ADCPs for the period from 8 to 30 July 2010.

Current Component Statistics	ECV	RME	r^2	Skill
Iona Island Surface Current	1%	-5%	0.88	0.94
Iona Island Bottom Current	1%	11%	0.86	0.91
Indian Point Surface Current	1%	-3%	0.88	0.95
Indian Point Bottom Current	1%	7%	0.85	0.93
Stony Point Surface Current	1%	4%	0.88	0.95
Stony Point Bottom Current	1%	10%	0.94	0.96
Average	**1%**	**5%**	**0.89**	**0.95**
Guidance	**10%**	**±30**	**0.94**	**0.92**

4.2.4 TEMPERATURE

Temperature comparisons between model predictions and observations are shown for pairs of surface and bottom thermistor station locations (east and west sides of the channel in the River) from the southernmost stations to the northernmost. The comparison is broken into three River sections: stations south of IPEC, those in the immediate IPEC area and stations north of IPEC.

Station to the south of IPEC include stations 58 and 64 at the southern end of the domain, stations 1 and 2 at mid-Haverstraw Bay, and stations 5 and 6 at the north end of Haverstraw bay. For the IP area, stations 9 and 10 are just north of Stony Point, stations 14 and 15 just south of IPEC, IPEC transect stations 29 and 27, and station 38 just north of IPEC. The stations further north of the IPEC area include stations 45 and 46 just south of Iona Island, stations 49 and 50 at Bear Mountain Bridge and finally stations 53 (coincident with West Point) and 54, at the northern end of the study domain.

4.2.4.1 STATIONS SOUTH OF IPEC

Stations 58 and 64 are the two southernmost thermistor mooring locations and just north of the open boundary area near Hastings on Hudson, with station 58 on the west side of the main channel and station 64 on the east. The temperature signals at stations 58 and 64 (see Figure 4-19 and Figure 4-20, respectively) were quite similar indicating little across-River variation at that transect (although a considerable amount of data is missing from the station 64 record), which was also seen in comparison of the model time series at the two stations.

Stations 1 and 2 represent the midpoint of Haverstraw Bay, approximately 14 mi north of the open boundary at Hastings on Hudson. The simulations at station 1 surface (Figure 4-21) generally track the observations closely, with a tendency to underestimate the peaks. The observations and model predictions at station 1 bottom compare well in terms of average daily temperature and both clearly respond to the semi-diurnal tidal variation, although the model was not quite as dynamic as the observations. Station 2, on the east side of the channel, showed a strong correlation to the observations capturing the semi-diurnal peaks seen in the surface record (Figure 4-22). The model predictions for the station 2 bottom record were very consistent with the observations from 16 July on, but tended to over predict temperatures early in the record. The model therefore captured the extent and distribution of the IPEC thermal plume in both timing and magnitude.

Stations 5 and 6 are located approximately 2 mi up-River from stations 1 and 2, with station 5 located on the west side of the main channel, and station 6 on the east. At station 5, the model results at the surface track the observations closely, with the model underestimating the observations during peak daily temperatures (Figure 4-23). The station 5 bottom record average model predicted temperatures compare well to those observed, although less dynamic. Station 6 surface temperatures generally follow the observed trends with the timing of peaks and troughs corresponding well. The station 6 bottom temperatures and trends compare well with observed with some differences before 16 July.

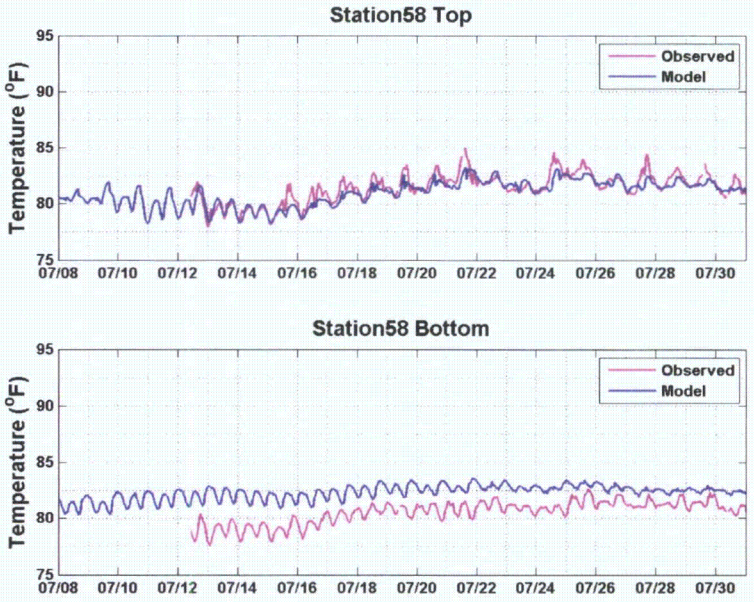

Figure 4-19. Near surface (upper panel) and near bottom (lower panel) temperature comparisons between model predictions (shown in blue) and observations (shown in pink) for the period from 8 through 30 July 2010 at station 58.

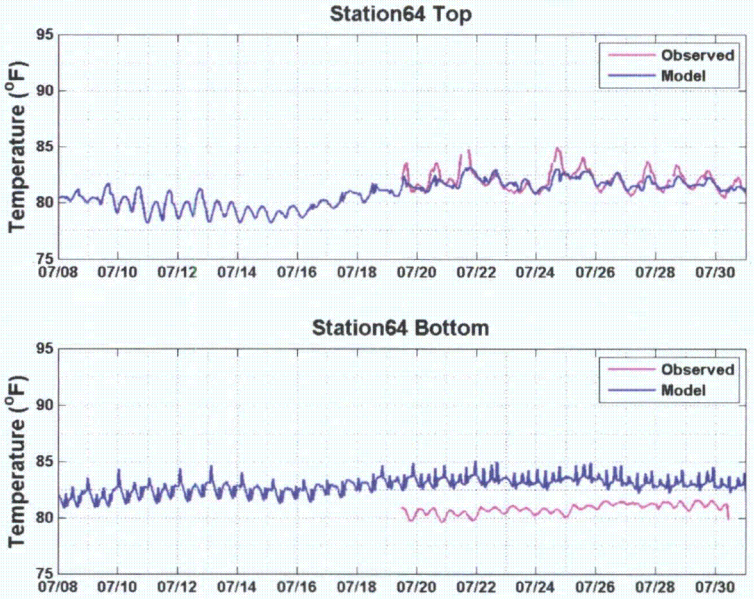

Figure 4-20. Near surface (upper panel) and near bottom (lower panel) temperature comparisons between model predictions (shown in blue) and observations (shown in pink) for the period from 8 through 30 July 2010 at station 64.

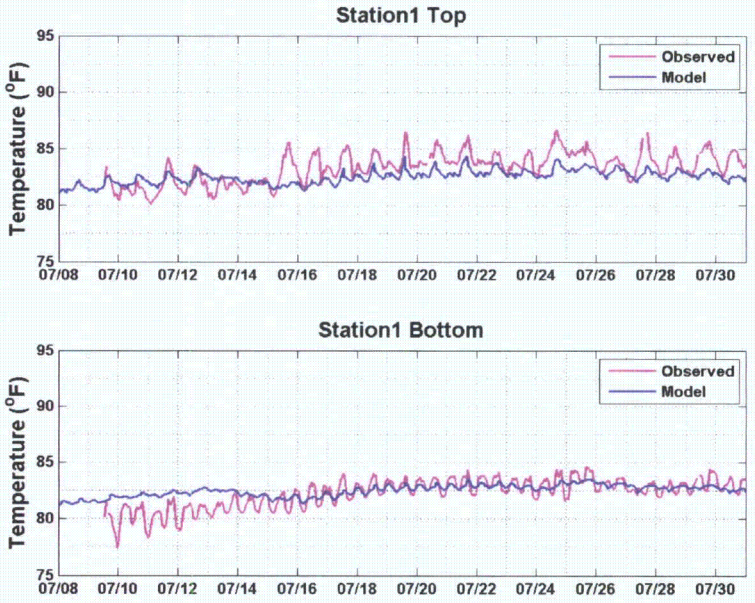

Figure 4-21. Near surface (upper panel) and near bottom (lower panel) temperature comparisons between model predictions (shown in blue) and observations (shown in pink) for the period from 8 through 30 July 2010 at station 1.

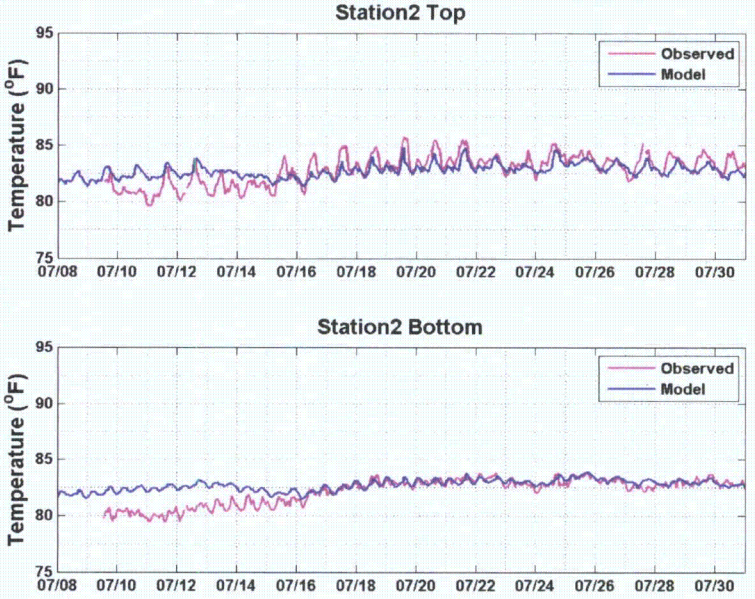

Figure 4-22. Near surface (upper panel) and near bottom (lower panel) temperature comparisons between model predictions (shown in blue) and observations (shown in pink) for the period from 8 through 30 July 2010 at station 2.

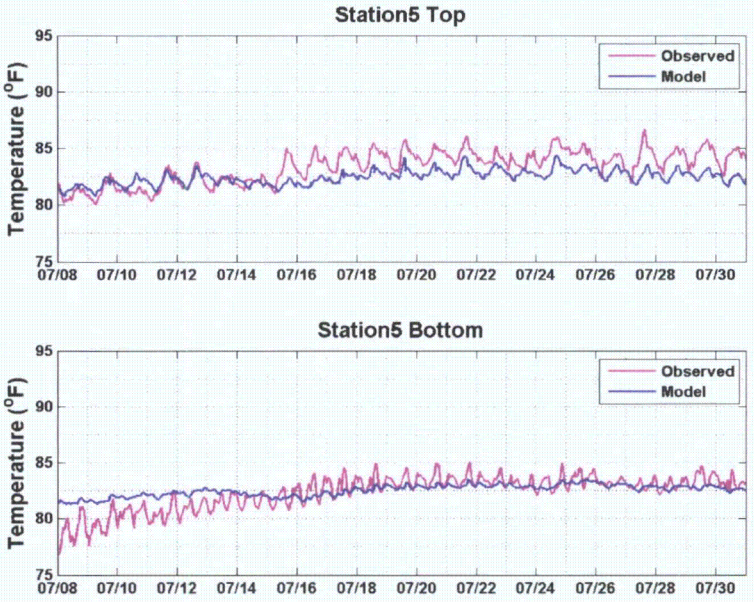

Figure 4-23. Near surface (upper panel) and near bottom (lower panel) temperature comparisons between model predictions (shown in blue) and observations (shown in pink) for the period from 8 through 30 July 2010 at station 5.

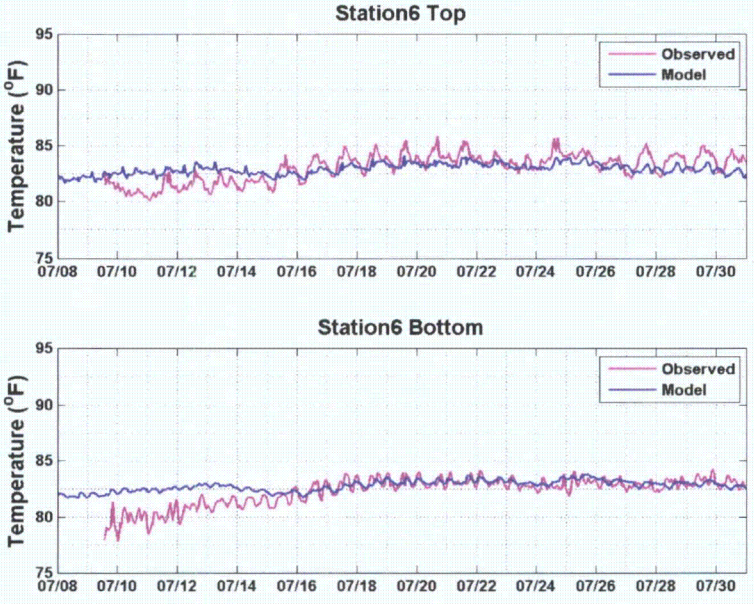

Figure 4-24. Near surface (upper panel) and near bottom (lower panel) temperature comparisons between model predictions (shown in blue) and observations (shown in pink) for the period from 8 through 30 July 2010 at station 6.

4.2.4.2 STATIONS IN THE IPEC AREA

Stations 9 and 10 are located approximately 2 mi upstream from stations 5 and 6, in the vicinity just north of Stony Point, with station 9 located on the west side of the main channel and station 10 on the east. The surface simulations at station 9 were close to the observations in terms of picking up semi-diurnal cycle well and closely mirror the observations, although the model results were typically somewhat cooler than observed (Figure 4-25). This underestimate of the temperature was also seen at the bottom layer at station 9. The surface and bottom temperatures at station 10 were somewhat different, however, clearly indicating a rising or falling temperature in phase with the tide at the surface in response to the IPEC thermal plume. The model results show that this tidal variability and plume tracking was simulated well by the model. The bottom record showed cooler temperatures than the surface at station 10, indicating a stratified system, which was also captured by the model predictions..

Stations 14 and 15 are located approximately 1 to 1.5 mi upstream from stations 9 and 10 and less than 0.5 mi south of IPEC, with station 15 located on the west side of the main channel and station 14 on the east. The observed surface and bottom temperatures at station 15 generally showed a similar trend, although the surface often had relatively short, small amplitude temperature excursions (Figure 4-27) that were not captured in the model predictions. The simulations at station 15 were close to the observations. The observed surface temperatures at station 14 were significantly different compared to station 15, indicating a clear semi-diurnal thermal response from the IPEC plume, in phase with the tide at the surface. The simulation generally captured this response, including the distinct difference between the surface and the bottom. The model tracked the observations well at the bottom of station 14, while the surface tracked the large amplitude excursions of the observations well for some of the period.

Stations 29 and 27 form a transect located on a straight line across the River from IPEC, approximately 1 mi up River from stations 14 and 15. Station 29 is located on the west side of the main channel, and station 27 on the east. There was a significant difference between the observed temperatures on the west side of the River (station 29) where the temperatures are lower than on the east side (station 27), which clearly reflected the presence of the plume. This difference was then a representation of the thermal plume geometry, concentrating on the east side of the river with a substantial drop in temperatures across the river. The plant effluent often exceeded 100°F at the discharge, but such high temperatures were significantly diminished (to approximately 85°F) by the time it reached station 27, approximately 900 ft from the discharge. This trend continued across the river to station 29 along the western side of the channel, where the influence from the thermal plume was only barely evident. This trend was well captured by the model-predicted temperatures, with a general decrease in predicted temperatures away from the discharge. Observed and model temperatures agreed well at station 27 with some underestimation by the model at station 29. The bottom temperatures tracked the observations well at each of the stations, although bottom thermistor 29 had a limited record.

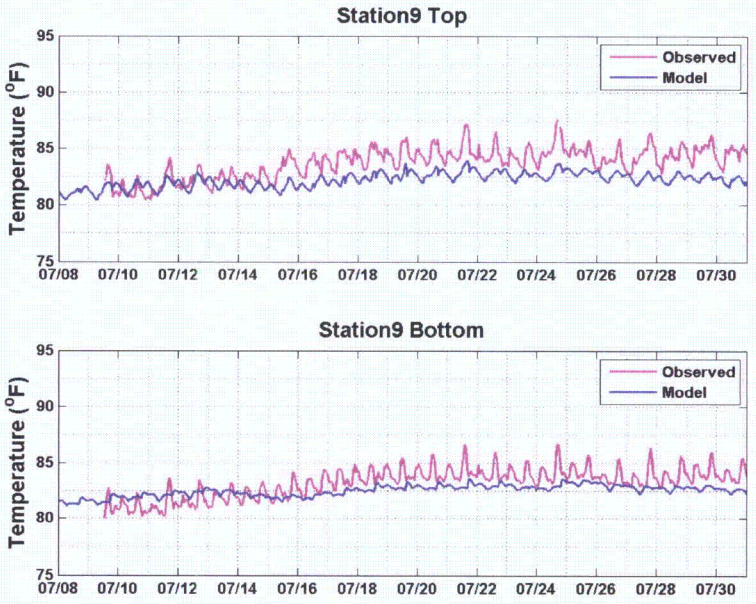

Figure 4-25. Near surface (upper panel) and near bottom (lower panel) temperature comparisons between model predictions (shown in blue) and observations (shown in pink) for the period from 8 through 30 July 2010 at station 9.

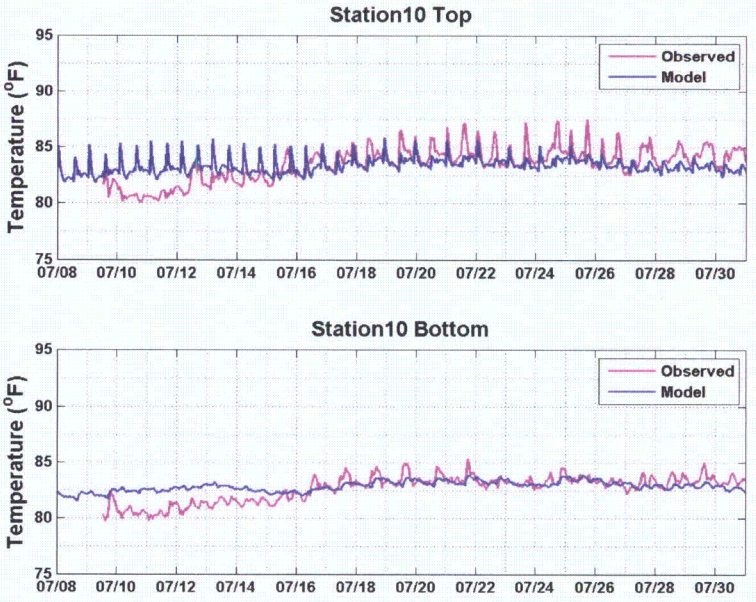

Figure 4-26. Near surface (upper panel) and near bottom (lower panel) temperature comparisons between model predictions (shown in blue) and observations (shown in pink) for the period from 8 through 30 July 2010 at station 10.

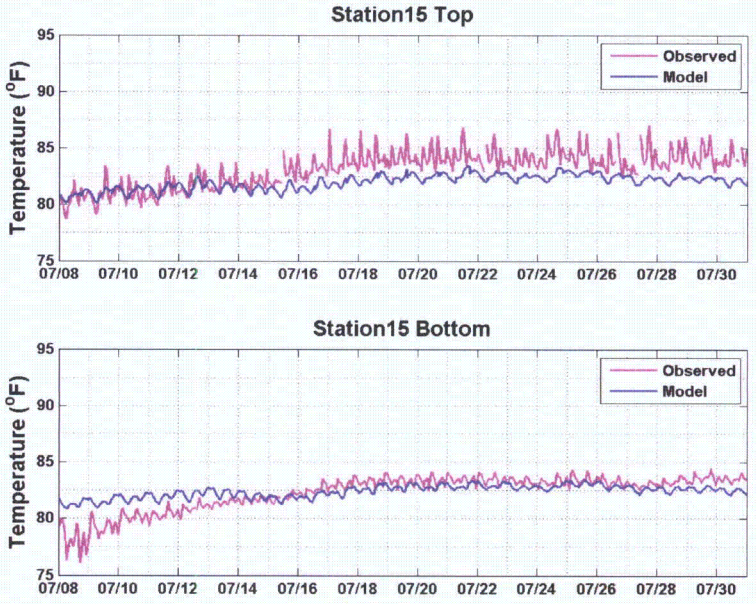

Figure 4-27. Near surface (upper panel) and near bottom (lower panel) temperature comparisons between model predictions (shown in blue) and observations (shown in pink) for the period from 8 through 30 July 2010 at station 15.

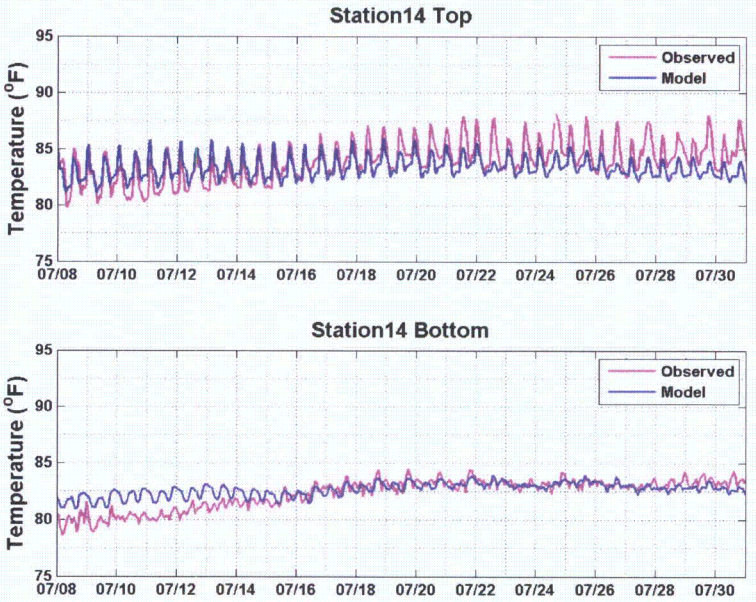

Figure 4-28. Near surface (upper panel) and near bottom (lower panel) temperature comparisons between model predictions (shown in blue) and observations (shown in pink) for the period from 8 through 30 July 2010 at station 14.

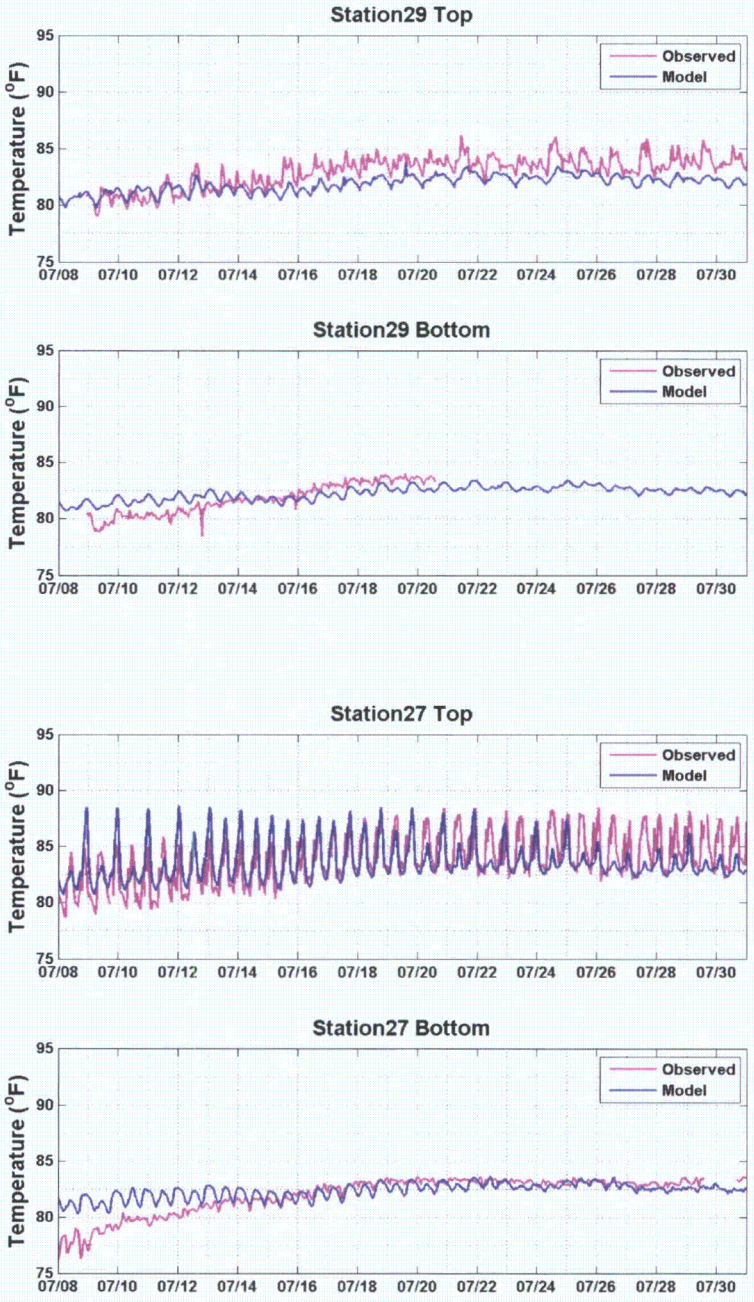

Figure 4-29. Near surface (upper panel) and near bottom (lower panel) temperature comparisons between model predictions (shown in blue) and observations (shown in pink) for the period from 8 through 30 July 2010 at station 29 27.

Finally, station 38 is located on the east side of the River channel approximately 0.5 mi up-River from the station 27 – 29 transect. There was a significant diminution of the thermal signal seen at station 38 when compared to station 27, just a short distance to the south (Figure 4-30). The model-predicted

surface temperatures closely tracked the observed temperatures for the first half of the study period but tended to diverge somewhat during the latter portion of the period. The bottom temperatures compared well during the latter part of the period after an initial over-prediction associated with atmospheric forcing affecting the river upstream. Overall the model results at station 38 compared adequately to the observed data. The surface model results for each of these stations missed the height of peaks during the flood tide, although the temperatures during the ebb tide corresponded well between observed and model simulations, and the phasing of the peaks and troughs between the model and observed data tracked well.

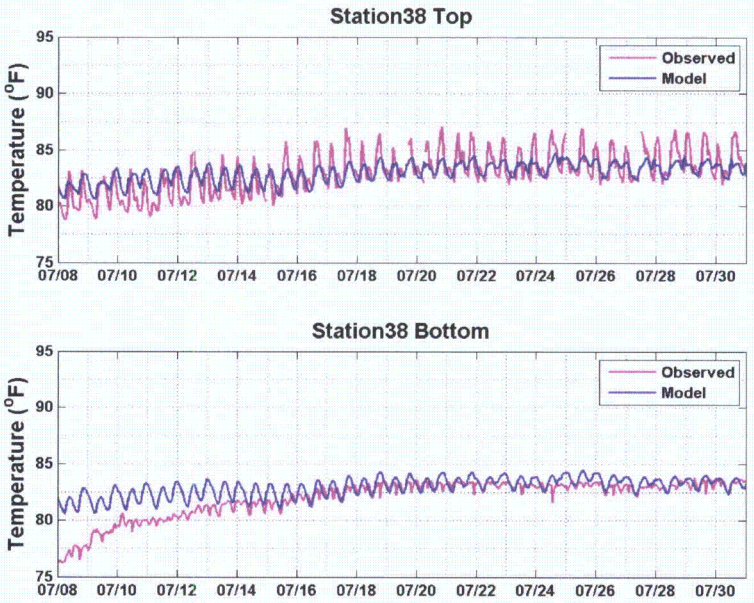

Figure 4-30. Near surface (upper panel) and near bottom (lower panel) temperature comparisons between model predictions (shown in blue) and observations (shown in pink) for the period from 8 through 30 July 2010 at station 38.

4.2.4.3 STATIONS NORTH OF IPEC

There are three sets of stations north of the Indian Point area, including pairs just south of Iona Island, at Bear Mountain Bridge and at West Point. Stations 45 and 46 are located approximately 1.5 to 2 mi up-River from station 38, with station 46 located on the west side of the main channel, and station 45 on the east. At this transect, the model-predicted surface and the bottom temperatures compared adequately with the observed data (Figure 4-31 and Figure 4-32), however, the simulated surface temperatures showed smaller semi-diurnal peaks than the observations at station 46.

Stations 49 and 50 are located approximately 4 mi up-River from IPEC just south of the Bear Mountain Bridge, with station 50 located on the west side of the main channel, and station 49 on the east. At these stations, the temperatures began to show a strong diurnal variability indicating that a significant amount of the response was due to the daily heating and cooling associated with the air temperature and solar radiation, with less influence from the transport of cooler or warmer waters during the ebb and flood tides (Figure 4-33 and Figure 4-34). Overall the model-predicted surface and bottom temperatures at both stations 49 and 50 compared well with the observed data, following both the trend and the diurnal fluctuations.

This diurnal response seen at these stations was even clearer at the north end of the 2010 study domain at stations 53 and 54 (Figure 4-35 and Figure 4-36, respectively) at West Point about 9 mi north of IPEC. At both stations 53 and 54 the surface temperatures very closely tracked the observations indicating that the model-predicted environmental forcing response was well represented. This also indicated that the model will perform well with the prediction of the environmental background, or ambient temperatures, used in the assessment of the IPEC thermal plume compliance with NYSDEC Thermal WQS.

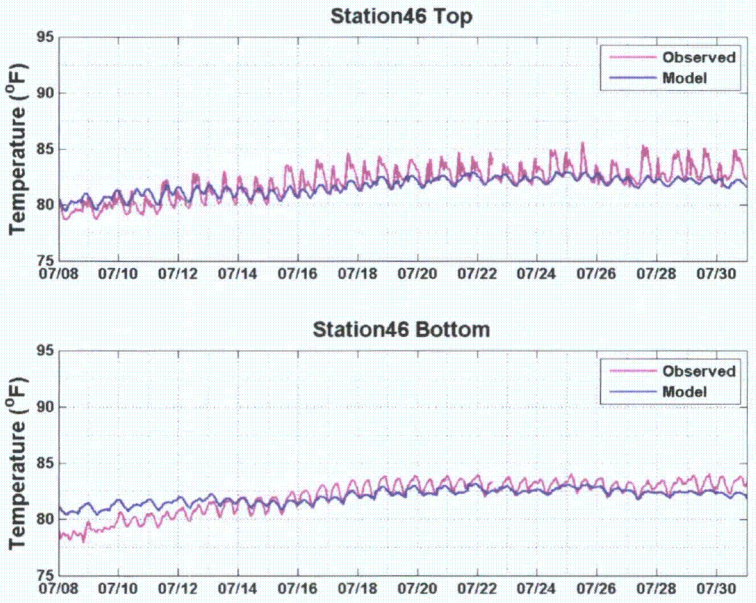

Figure 4-31. Near surface (upper panel) and near bottom (lower panel) temperature comparisons between model predictions (shown in blue) and observations (shown in pink) for the period from 8 through 30 July 2010 at stations 45 and 46.

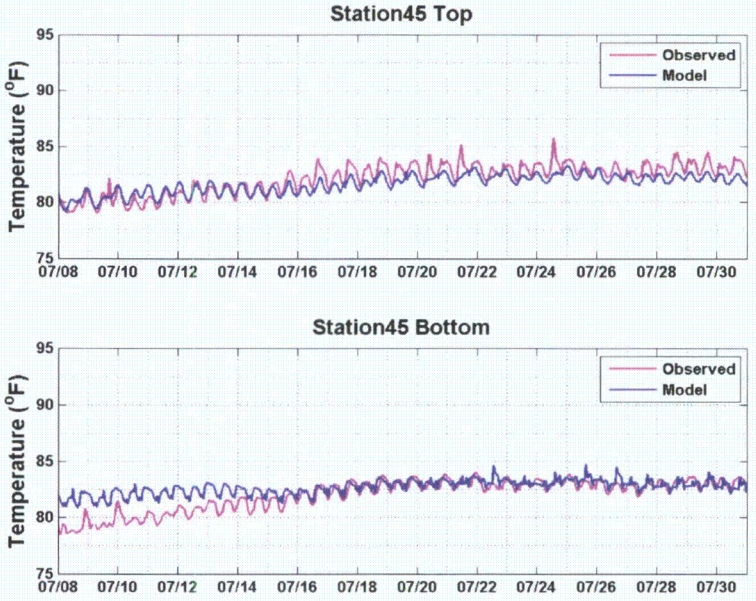

Figure 4-32. Near surface (upper panel) and near bottom (lower panel) temperature comparisons between model predictions (shown in blue) and observations (shown in pink) for the period from 8 through 30 July 2010 at stations 45 and 46.

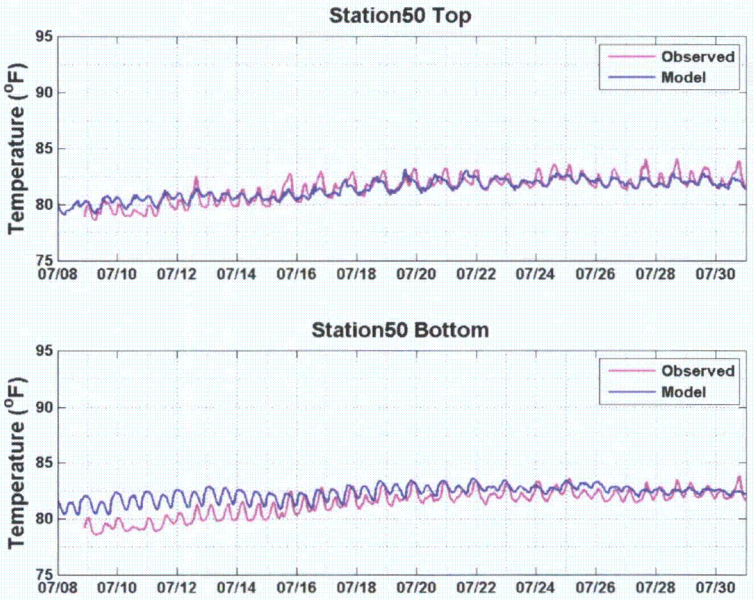

Figure 4-33. Near surface (upper panel) and near bottom (lower panel) temperature comparisons between model predictions (shown in blue) and observations (shown in pink) for the period from 8 through 30 July 2010 at station 50.

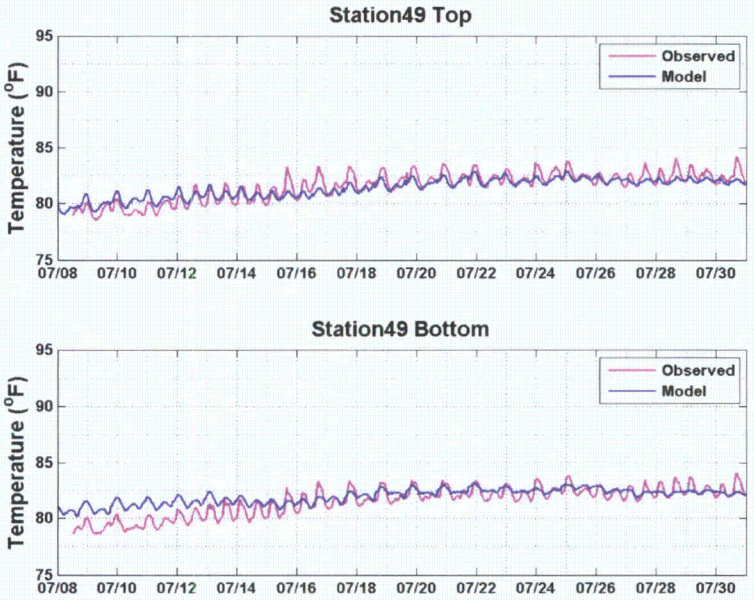

Figure 4-34. Near surface (upper panel) and near bottom (lower panel) temperature comparisons between model predictions (shown in blue) and observations (shown in pink) for the period from 8 through 30 July 2010 at station 49.

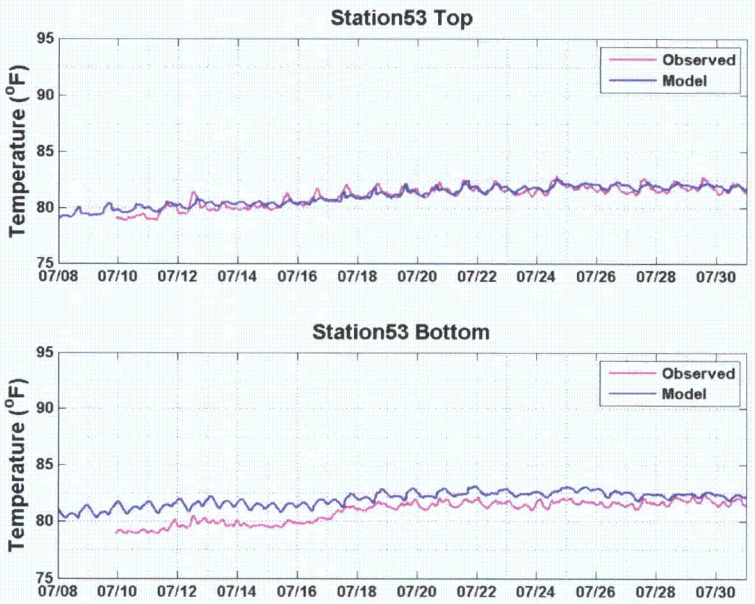

Figure 4-35. Near surface (upper panel) and near bottom (lower panel) temperature comparisons between model predictions (shown in blue) and observations (shown in pink) for the period from 8 through 30 July 2010 at station 53.

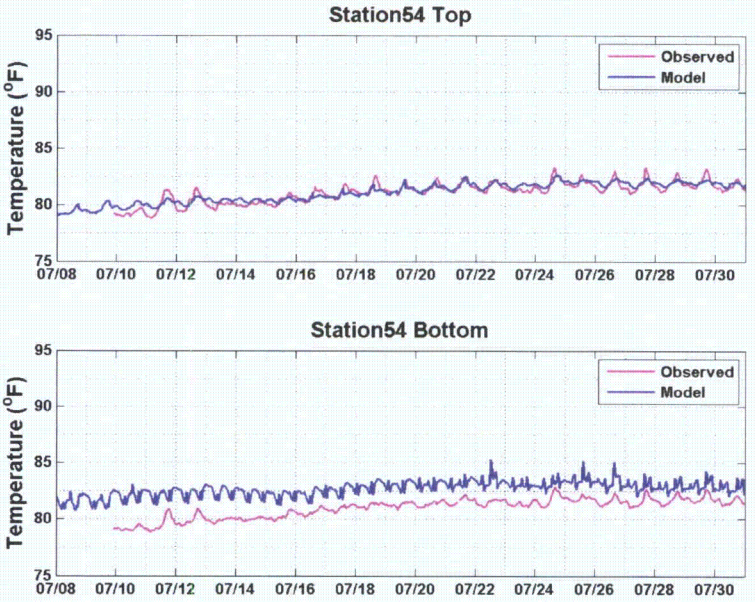

Figure 4-36. Near surface (upper panel) and near bottom (lower panel) temperature comparisons between model predictions (shown in blue) and observations (shown in pink) for the period from 8 through 30 July 2010 at station 54.

4.2.4.4 STATISTICAL ANALYSIS

The parameters presented in Table 4-4 are measures of model prediction to observations statistical differences. The parameters include: relative mean error (RME), error coefficient of variance (ECV), and squared correlation coefficient, r^2. Also presented in each table are the average values of each measure and the USEPA guidance levels for each statistical measure. In addition model "skill" was calculated for each data set.

Squared correlation coefficients between the temperature prediction and observation vary over the study domain. The spatial average with this correlation was 0.59, which is lower than the USEPA guidance level of >0.84. RME for the temperature predictions ranges was between -1% and 2%, with an average of 0.1%, well below the USEPA guidance level of <25%. ECV varied from 1% (at many stations) to 2%, with an average of 1.4%, compared to the guidance level of <45%. The temperature RME and ECV values are much smaller than the guidance levels, implying that the model predicted the surface temperature well. On average, the skill level of 0.74 was slightly less than the guidance level of >0.85. The range of temperature variation during the 2010 validation modeling period was smaller than the 2009 calibration period (Swanson et al., 2010b) and thus the variance and standard deviation were smaller, which resulted in relatively lower values for the squared correlation coefficients and Skill. The statistics also showed that the model did equally well for the surface and the bottom predictions, with no difference in the correlation coefficient and only minor variations in the others.

The statistical measures were calculated at individual locations using model predictions and field observations on an hourly basis. The result was a rigorous and detailed assessment of the differences between the model predictions and observations on a time dependent basis. While these statistics are commonly used for this type of model calibration and validation study for scientific assessment, the purpose of this application is to understand the potential impacts of the IPEC thermal plume on a spatial basis where the timing is of no importance. The comparison of the model-predicted surface and bottom temperatures to the observations on both a qualitative (time series and plume transport map plots) and quantitative basis (statistics presented here) show that the model predicts the location and spatial dynamics of the plume, the key quantity necessary for the assessment of the regulatory criteria.

Table 4-4. Quantitative comparisons of predicted and observed temperatures for surface and bottom thermistors at selected stations for the validation period.

Station	Location	R2	RME	ECV	Skill
1	Surface	0.45	1.0%	2.0%	0.63
1	Bottom	0.49	0.0%	1.0%	0.61
2	Surface	0.44	0.0%	1.0%	0.67
2	Bottom	0.5	1.0%	1.0%	0.63
5	Surface	0.56	1.0%	2.0%	0.67
5	Bottom	0.59	0.0%	1.0%	0.64
6	Surface	0.36	0.0%	1.0%	0.58
6	Bottom	0.38	1.0%	1.0%	0.55
9	Surface	0.4	2.0%	2.0%	0.57
9	Bottom	0.36	1.0%	2.0%	0.6

Station	Location	R2	RME	ECV	Skill
10	Surface	0.21	0.0%	2.0%	0.54
10	Bottom	0.37	1.0%	1.0%	0.58
15	Surface	0.55	1.0%	2.0%	0.65
15	Bottom	0.64	0.0%	1.0%	0.71
14	Surface	0.44	1.0%	2.0%	0.7
14	Bottom	0.61	0.0%	1.0%	0.73
29	Surface	0.62	1.0%	2.0%	0.68
29	Bottom	0.61	0.0%	1.0%	0.7
27	Surface	0.34	0.0%	2.0%	0.73
27	Bottom	0.5	0.0%	2.0%	0.66
38	Surface	0.59	0.0%	2.0%	0.75
38	Bottom	0.55	1.0%	2.0%	0.71
46	Surface	0.71	0.0%	1.0%	0.8
46	Bottom	0.83	0.0%	1.0%	0.83
45	Surface	0.77	1.0%	1.0%	0.85
45	Bottom	0.83	0.0%	1.0%	0.87
50	Surface	0.77	0.0%	1.0%	0.9
50	Bottom	0.85	0.0%	1.0%	0.91
49	Surface	0.79	0.0%	1.0%	0.89
49	Bottom	0.83	0.0%	1.0%	0.9
53	Surface	0.83	0.0%	1.0%	0.94
53	Bottom	0.88	0.0%	1.0%	0.91
54	Surface	0.83	0.0%	1.0%	0.94
54	Bottom	0.85	0.0%	1.0%	0.92
58	Surface	0.76	0.0%	1.0%	0.91
58	Bottom	0.76	1.0%	1.0%	0.88
64	Surface	0.53	0.0%	1.0%	0.76
64	Bottom	0.01	1.0%	1.0%	0.35
65	Surface	0.72	1.0%	1.0%	0.84
65	Bottom	0.34	1.0%	2.0%	0.64
66	Surface	0.85	1.0%	1.0%	0.93
66	Bottom	0.61	1.0%	2.0%	0.8
	Surface Average	**0.6**	**0.5%**	**1.4%**	**0.76**
	Bottom Average	**0.59**	**0.4%**	**1.2%**	**0.72**
	Average	**0.59**	**0.5%**	**1.3%**	**0.74**
	Guidance	**0.84**	**± 25**	**45%**	**0.85**

5 Model Results Compared To NYSDEC Thermal Criteria

5.1 NYSDEC Thermal Criteria

The NYSDEC criteria governing thermal discharges found in 6 NYCRR § 704, specifically § 704.2, includes categorical or general criteria governing all waters receiving thermal discharges, and specific criteria for estuaries or parts of estuaries [704.2 (b) (5)]. There are four specific criteria:

(i) The water temperature at the surface of an estuary (i.e., beyond the inferred mixing zone) shall not be raised to more than 90°F at any point.

(ii) At least 50% of the cross sectional area and/or volume of the flow of the estuary including a minimum of 1/3 of the surface as measured from water edge to water edge at any stage of tide, shall not be raised to more than 4°F over the temperature that existed before the addition of heat of artificial origin or a maximum of 83°F whichever is less.

(iii) From July through September, if the water temperature at the surface of an estuary before the addition of heat of artificial origin is more than 83°F an increase in temperature not to exceed 1.5°F at any point of the estuarine passageway as delineated above, may be permitted.

(iv) At least 50% of the cross sectional area and/or volume of the flow of the estuary including a minimum of 1/3 of the surface measured from water edge to water edge at any stage of the tide, shall not be lowered more than 4°F from the temperature that existed immediately prior to such lowering.

5.2 Model Results Processing For Compliance Evaluation

Compliance with the applicable Thermal WQS was assessed using the Model predictions for the 8 through 30 July 2010 validation period. The processing of Model results included determination of the spatial extent of any water over 90°F from the IPEC thermal discharge (beyond the inferred mixing zone), determination of the applicable plume temperature rise criteria (1.5°F vs. 4°F per (iii) above) and the subsequent spatial delineation of the 1.5°F (if applicable) and 4°F thermal plume extents from the IPEC thermal discharge at nine different cross sections. The following subsections describe the processing performed.

5.2.1 Spatial Extent of 90°F

Determination of the spatial extent of predicted water temperatures exceeding 90°F due to IPEC discharge was made by tracking all the model grid cell surface areas with predicted surface temperatures above 90°F for each time step of the simulation. This calculation included model grid cells that fell within the inferred mixing zone.

5.2.2 Determination of Applicable Temperature Criteria

The water quality standards invoke different limits (1.5°F or 4°F) to the allowable temperature rise above ambient based on an ambient water temperature of 83°F during July through September. If ambient temperatures are less than 83°F then the allowable plume increment is 4°F while if the ambient temperatures are above 83°F then the allowable plume increment is 1.5°F. Ambient temperature is defined as the temperature that existed before the addition of heat of artificial origin. Ambient

temperatures were determined using the model predictions of temperatures during the period without thermal loading from power plants in the system. Model predictions are used as a reference because ambient temperatures cannot be measured due to the presence of artificial heat sources (plant loads) in the river at all times during the study period. The time varying ambient temperature predicted at a model grid cell close to IPEC (same locations as thermistor station 27) was used as a proxy for natural ambient in the region during the simulation.

5.2.3 Determination of Spatial Extent of Thermal Plume

Thermal WQS define allowable limits of vertical cross section area as well as surface width across the River of the thermal plume extent, with the allowable increment of temperature rise associated with the thermal plume relative to the natural ambient as described above. In order to estimate the actual incremental rise, the model results from a simulation run without thermal loads from any power plants were subtracted from the model results from a simulation with the thermal loads from IPEC and other power plants. The processing determined the temperature differential for each grid cell at every timestep of the model simulation, thus isolating the combined plant thermal contribution above ambient conditions.

This relative temperature rise above ambient was then further processed at multiple transects to determine the predicted extent of the 4°F thermal plume using the cell geometry and predicted temperatures. These results were evaluated to determine either if the 67% cross-River distance or 50% cross sectional area requirements were in compliance. The nine transects chosen for evaluation of these metrics span locations extending 1.5 mi (N3) upstream and 2.6 mi (S5) downstream from IPEC as shown in Figure 5-1. For those times when the ambient temperature exceeds 83°F the processing is repeated using the predicted extent of the 1.5°F thermal plume as defined by cross section and surface width. As shown below, the temperature threshold was not reached, so the 1.5°F thermal plume was not determined.

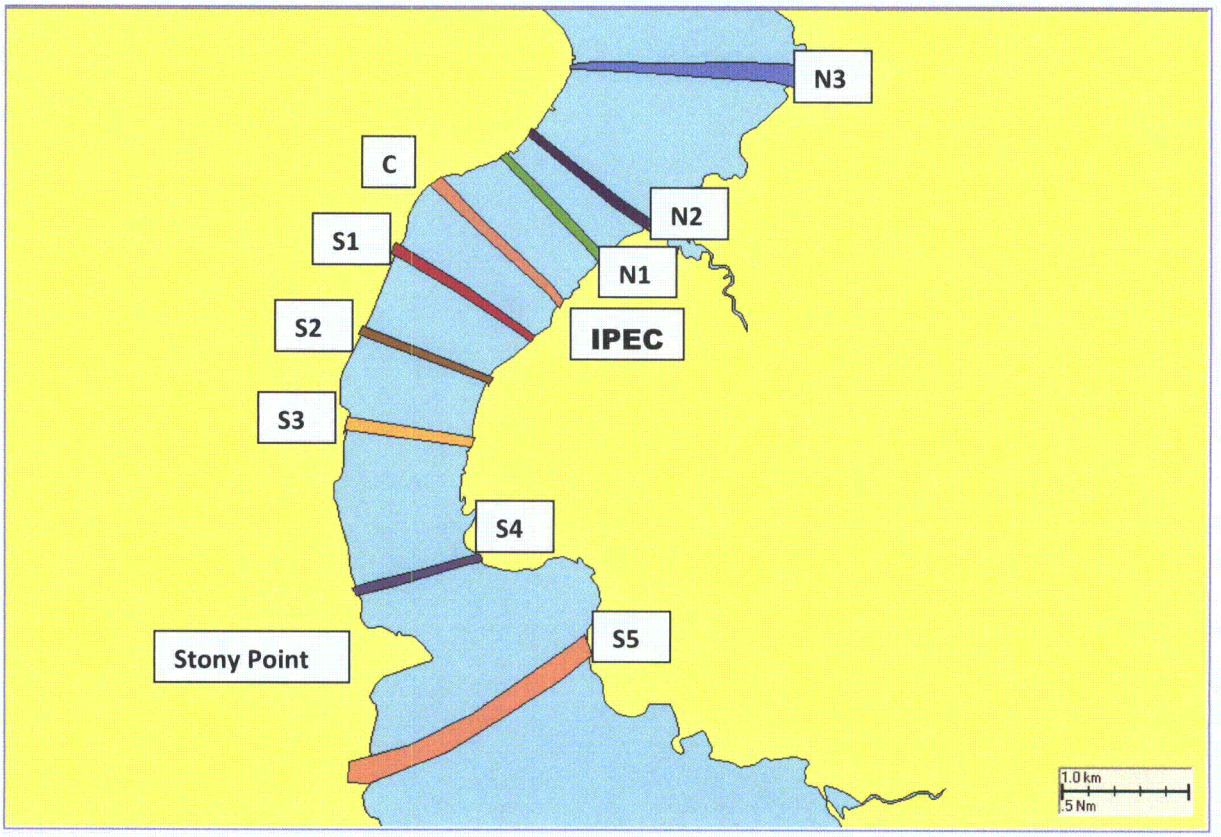

Figure 5-1. Location of river cross sections used to determine compliance with NYSDEC water quality standards (thermal criteria).

5.3 Compliance Evaluation of 2010 Summer Validation Period

The 8 through 30 July 2010 validation period model results were first post-processed to determine if the model predicted the occurrence of water temperature in the estuary (that included the inferred mixing zone) greater than 90°F. The results of the analysis, presented in Figure 5-2, showed that the variation of the surface area coverage of the 90°F was predominantly semi-diurnal (tidally driven), and averaged 2.2 acres (ac) over the simulation. There were two short term events seen in the record, which peaked at 14.6 ac. These peaks occurred during early ebb tide when the slack water pooling of warmer waters at the outfall was carried downstream. Most of the peaks were between 4 ac and 5 ac in size while a smaller set ranged between 5 and 14 ac. These areas were smaller than the 2005 extreme environmental condition results (Swanson et al., 2010b) which found a maximum area of under 35 ac and was typically less than 20 ac. The area coverage for temperatures greater than 90°F complies with the NYSDEC Thermal WQS by definition, based on the IPEC permit condition of a formulaic inferred mixing zone.

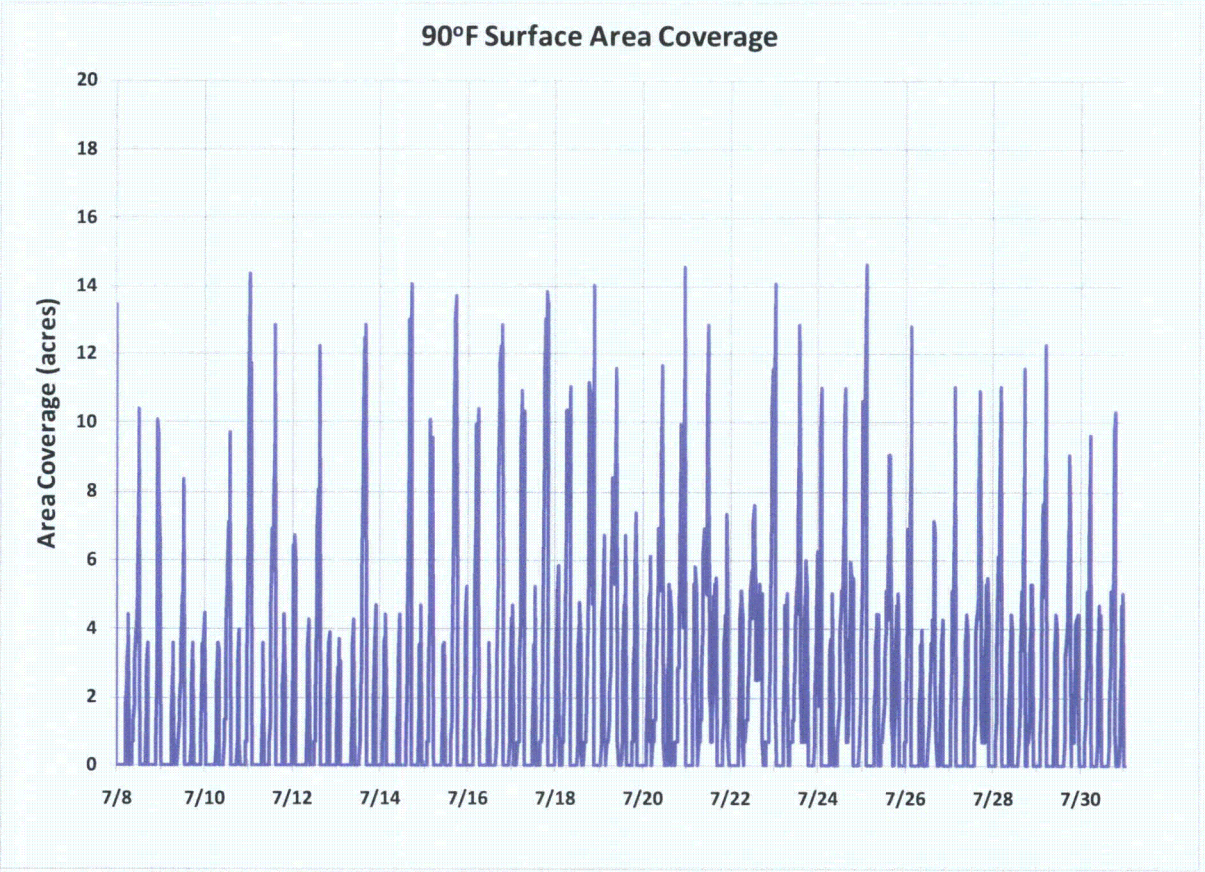

Figure 5-2. Surface area of temperatures greater than 90°F during the period from 8 through 30 July 2010.

Figure 5-3 shows a plan view of the model predicted surface water temperatures greater than 90°F during one of the largest events (14.6 ac), which occurred at 2300 on 20 July 2010. The area greater than 90°F is shown in the green area starting at IPEC extending downstream along the eastern shore. This area compares favorably with the area that encloses those fixed thermistor stations that recorded a temperature greater than 90°F. That area was approximately 26 ac but because the calculated area was based on the maximum thermistor temperature over the entire field program it included both flood and ebb conditions. The thermistors exceeding 90°F included stations 17, 21, 23, 24, 25, and 26. The numbered red icons are the thermistor locations. The vertical section view insert showed that the plume is restricted to the surface. This area would fall within an inferred mixing zone.

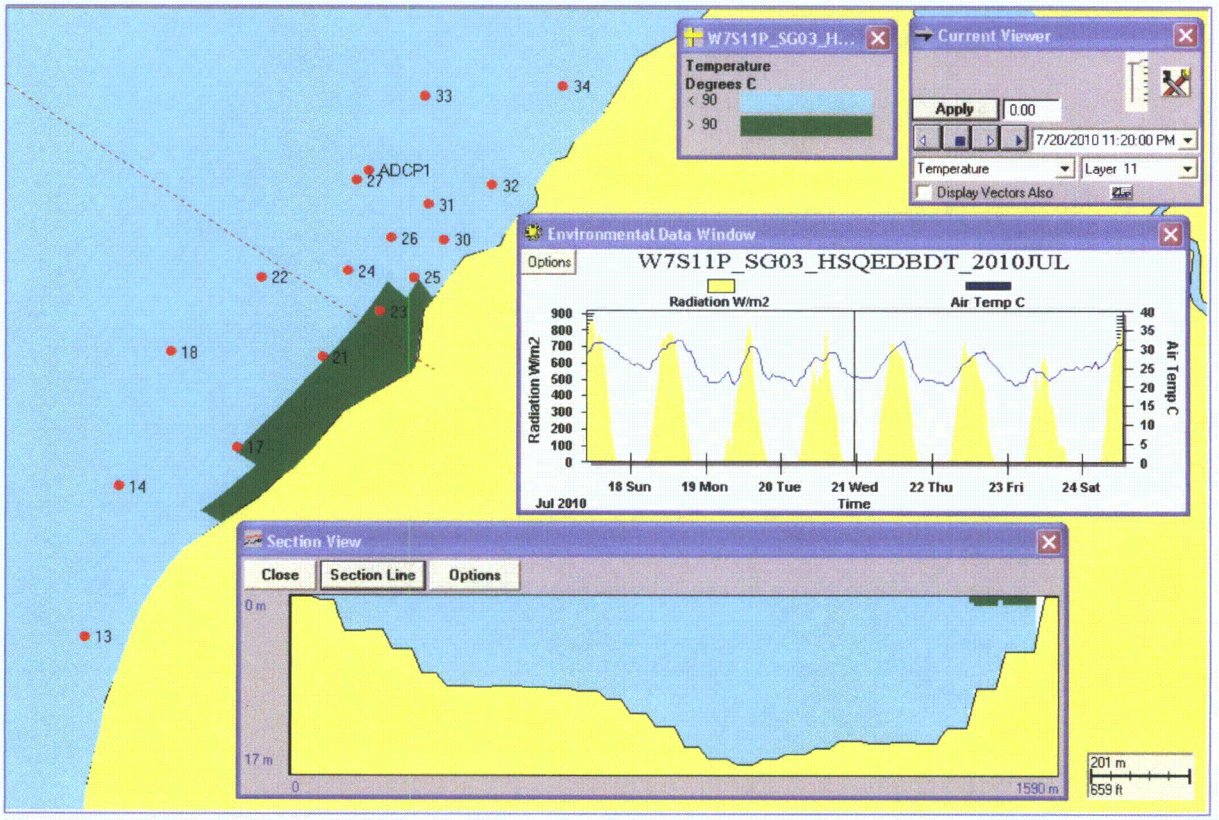

Figure 5-3. Plan view of one of the largest surface area coverage greater than 90°F occurring at 2300 on 20 July 2010.

The shape of the area greater than 90°F varies over the tidal cycle as well. Figure 5-4 shows the area at slack before ebb where the area has no upstream or downstream orientation. The time of slack water is relatively short, however, and the plume will quickly distend following the tide, in this case downstream with ebb tide. The area greater than 90°F shown in Figure 5-4 would fall within the inferred mixing zone.

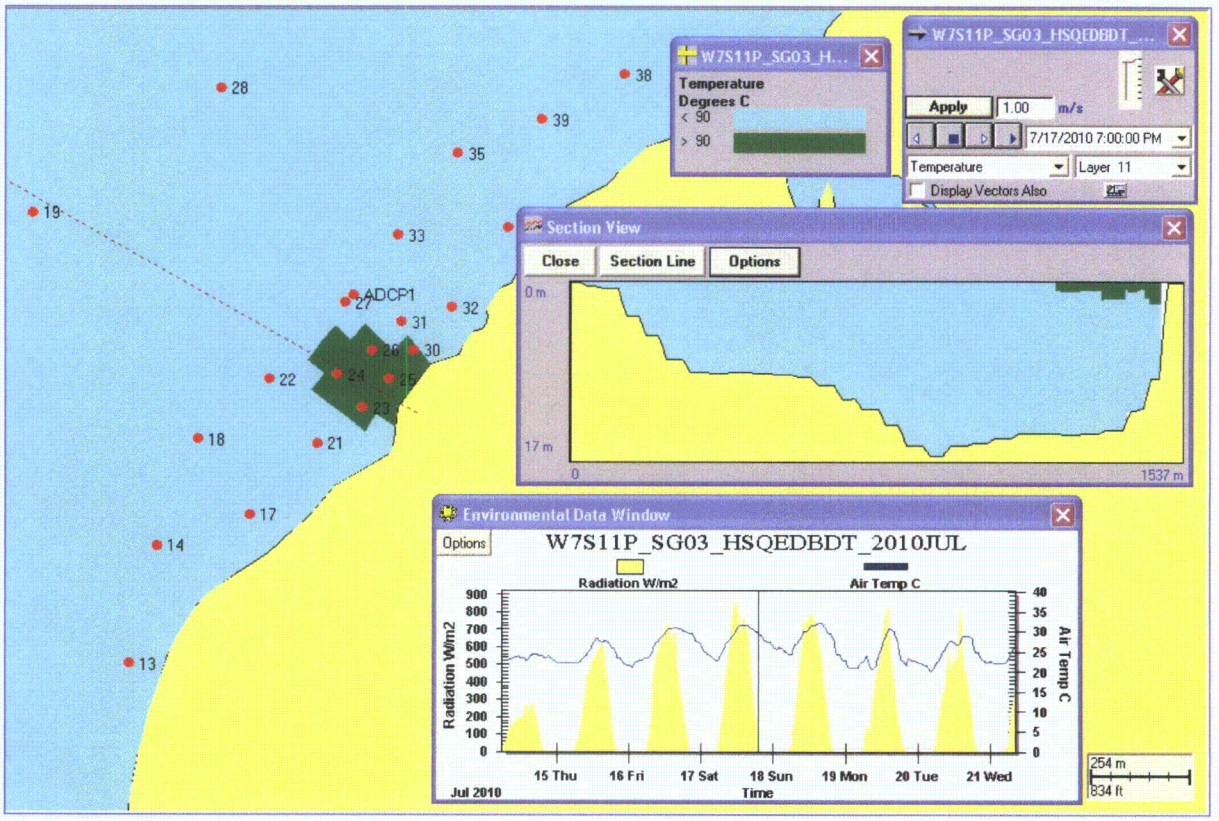

Figure 5-4. Plan view of surface area coverage greater than 90°F occurring at slack before ebb at 1900 on 17 July 2010.

The 8 through 30 July 2010 period results were processed to determine the natural ambient temperature close to the plant. Following the procedure described in the earlier modeling report (Swanson et al., 2010b) the model was run with no thermal discharges from any plant. Thermistor station 27 was used as a proxy for the ambient temperature; the predicted ambient temperatures for that period are shown in Figure 5-5. The surface ambient temperature reached a maximum of 82.2°F, always under the 83°F threshold where the allowable plume temperature rise is limited to 1.5°F versus the 4°F. Therefore, only the spatial extent of the cross sectional area and surface width of the 4°F were calculated to determine compliance.

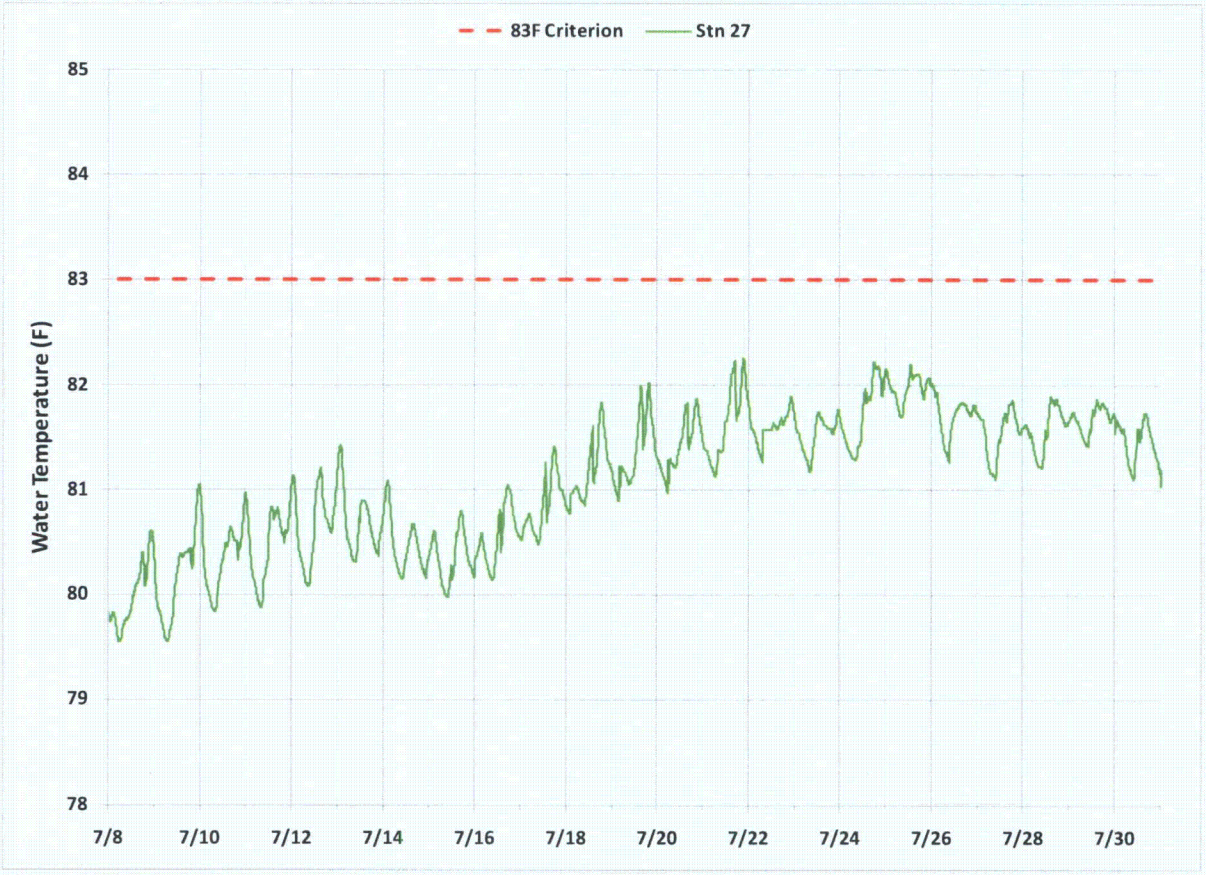

Figure 5-5. Surface temperature under ambient conditions (no plant loads) at station 27 during the 8 through 30 July 2010 period. The regulatory temperature threshold is shown as a dashed line.

In order to estimate the 4°F temperature rise, the model results based on no thermal loads from any power plants (the ambient condition) were subtracted from the model results based on the thermal loads from IPEC and other power plants. The processing determined the temperature differential for each grid cell at every timestep of the model simulation, thus isolating the combined plant thermal contribution above ambient conditions.

The area having a 4°F or greater temperature rise varies with the tides, at both semi-diurnal and spring-neap frequencies (12.42 hrs and 14.5 days, respectively), and other environmental and plant conditions. **Figure 5-6** shows a series of isotherms defining surface areas greater than 4°F ΔT from the model results for eight times through a tidal cycle. This tidal cycle was chosen because it shows the largest area. Also shown is the NYSDEC Thermal WQS surface width limit of 67% of the River width measured from the eastern shore. All the areas are anchored to the IPEC discharge and are oriented upstream or downstream with respect to the stage of the tide. The Max Flood area starts at the discharge and extends upstream. At Slack Before Ebb the area has moved back closer to the IPEC discharge. At both 1hr After Slack Before Ebb and 2hr After Slack Before Ebb the areas extend from the IPEC discharge downstream along the eastern shore of the River. At Max Ebb the area is no longer continuous, showing an area near the IPEC discharge and another approximately 1 mi downstream. Just previous to this time in the tidal cycle the downstream area was not as far south and still connected to the other area. At 1hr Before Slack Before Flood the area has diminished and is located near to and just downstream of the IPEC discharge. At Slack Before Flood the area is centered at the IPEC discharge and at 1 hr Before Slack Before Ebb the area is located at and just upstream of the IPEC discharge. In summary the area is much smaller during the flood tide compared to the much larger on ebb tide.

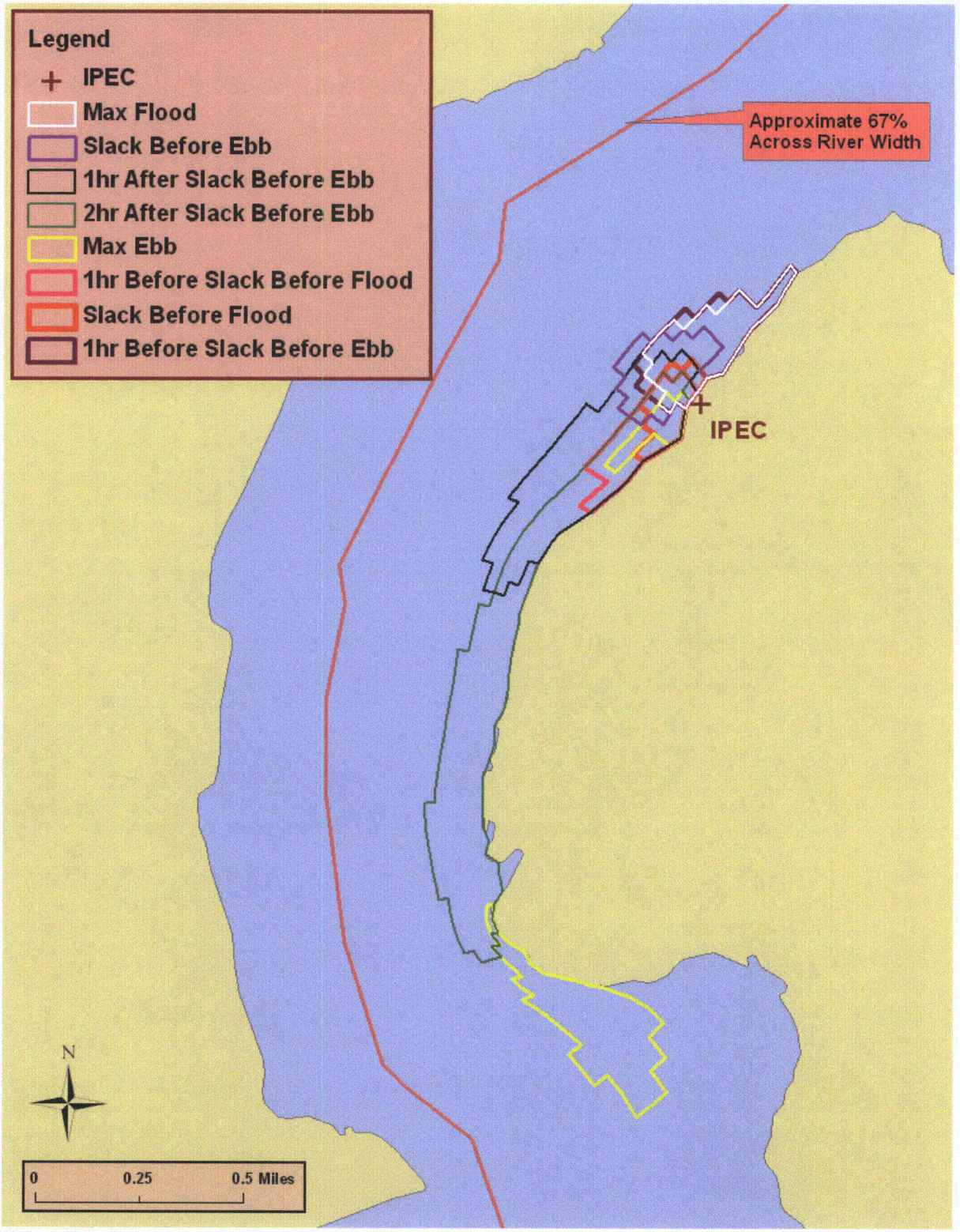

Figure 5-6. Variation of 4°F ΔT area at IPEC at different stages of the tidal cycle. The 67% surface width Thermal WQS limit is also shown.

Figure 5-7 shows the percent surface width for a 4°F temperature rise for the transects shown in Figure 5-1. Figure 5-7 shows that the 4°F surface plume generally repeats itself with tidal cycle regularity at all the cross sections.

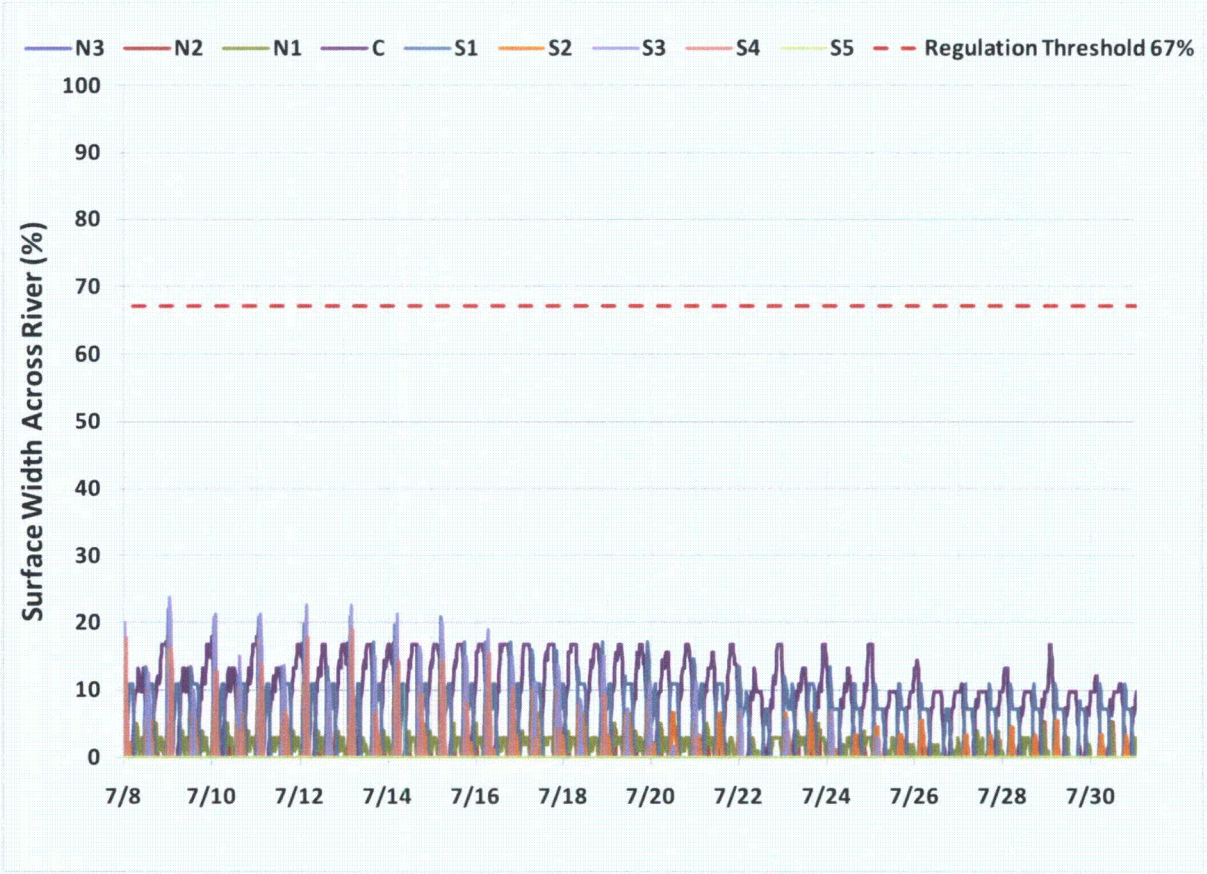

Figure 5-7. Surface width percentage based on a ΔT of 4°F for all sections during the period from 8 through 30 July 2010. The regulatory threshold of 67% is shown as a dashed line.

Table 5-1 shows the mean and maximum surface width percentages for each of the nine cross sections in the River (Figure 5-1). The maximum surface width occurs at section S3 (23.9%) with the center and four of the five southern sections somewhat lower (~18 – 22%). Two of the three northern sections show much smaller maxima (~5%). The northernmost (N3) and southernmost (S5) sections have zero maxima indicating the 4°F temperature rise does not reach those sections. The largest mean percentage occurs at the IPEC section (C) at 9.8% followed by the four southern sections (S1, S2, S3 and S4) between 4.9 and 8.6%. The two northern section means are much lower at 2.3 to 2.8%.

Table 5-1. Summary of surface width percentages of total River width at nine cross sections evaluated.

Transect	Mean (%)	Maximum (%)
N3	0.0	0.0
N2	2.8	5.2
N1	2.3	5.0
C	9.8	17.9
S1	8.3	22.0
S2	4.9	18.8
S3	8.6	23.9
S4	7.5	18.9
S5	0.0	0.0

Figure 5-8 shows the percent of the vertical cross sectional area covered for a 4°F temperature rise for the transects shown in Figure 5-1. Figure 5-8 shows that the 4°F cross sectional area coverage generally repeats itself with tidal cycle regularity at all of the cross sections. Throughout the entire validation period there is no section where the cross-sectional area exceeds 8%, well below the 50% limit.

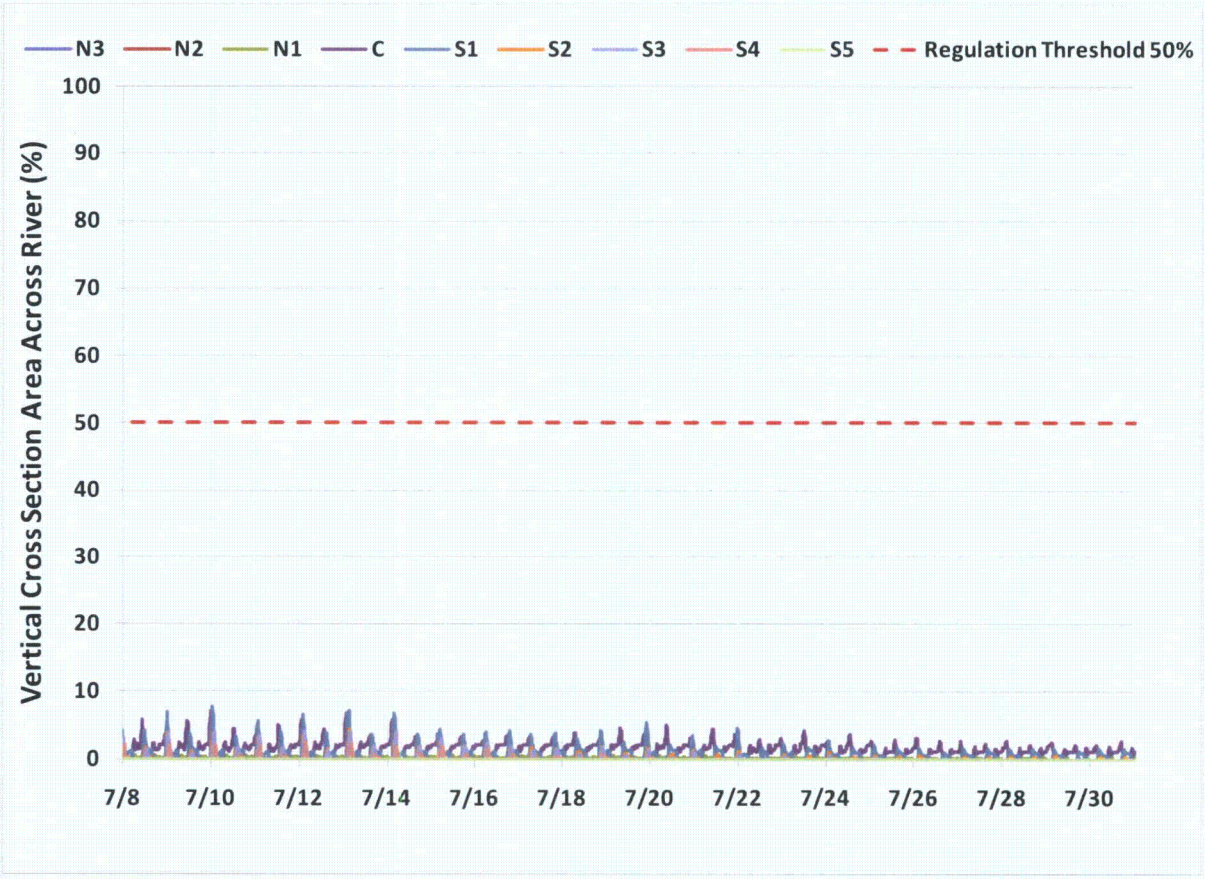

Figure 5-8. Vertical cross section area percentage based on a ΔT of 4°F for all sections during the period from 8 through 30 July 2010. The regulatory threshold of 50% is shown as a dashed line.

Table 5-2 shows the mean and maximum vertical cross section area percentages for each of the nine cross sections in the River (Figure 5-1). The maximum area occurs at section S1 (7.8%) followed closely by the center section (7.1%). Three of the five southern sections are somewhat lower (~2.4-4.3%). Two of the three northern sections show much smaller maxima (~0.5%). The northernmost (N3) and southernmost (S5) sections have zero maxima indicating the 4°F temperature rise does not reach those sections. The largest mean percentage occurs at the IPEC section (C) at 1.6% followed by the center (C) and four southern sections (S1, S2, S3 and S4) between 0.6 and 1.2%. The two northern section means are lower at 0.2%.

Table 5-2. Summary of vertical cross section area percentages of total River vertical cross section area at nine cross sections evaluated.

Transect	Maximum (%)	Mean (%)
N3	0.0	0.0
N2	0.4	0.2
N1	0.6	0.2
C	7.1	1.6
S1	7.8	1.2
S2	4.3	0.6
S3	4.1	1.1
S4	2.4	0.8
S5	0.0	0.0

The analysis shows that IPEC is within compliance of the NYSDEC Thermal WQS during the validation period, 8 through 30 July 2010. There is a small area (14.6 ac) of the River near the IPEC discharge that exceeds 90°F but that it is compliant with the inferred mixing zone of the discharge. The maximum ambient temperature during the period was 82.2°F, which is under the temperature threshold requiring the use of the 1.5°F temperature rise criteria. The 4°F temperature rise reached a maximum of 23.9% of the River width and 7.8% of the River vertical cross section area, well under the Thermal WQS limits of 67% for width and 50% for area.

To assess the sensitivity of the model results the analysis was repeated assuming that the ambient temperature was 1°F warmer than calculated. Under this assumption the maximum ambient exceeded the 83°F threshold so the 1.5°F ΔT isotherm was used to calculate surface width and vertical cross section area. Neither measures exceeded the Thermal WQS limits of 67% for width and 50% for area under the assumed conditions.

6 CONCLUSIONS

This report describes the methodology and results of a triaxial thermal study that consisted of a combination of field work conducted in summer of 2010 and subsequent hydrothermal modeling. The report expands on an earlier (late summer – early fall 2009) thermal field and modeling program (Swanson et al., 2010b). These conclusions focus first on the findings of the 2010 field program; model results for the simulation period (8 – 30 July 2010), and post processing of the model results to establish if the IPEC discharge complies with the NYSDEC Thermal WQS.

6.1 2010 FIELD MONITORING PROGRAM

The 2010 Field Program, consisting of a fixed extensive observation array and mobile surveys, was performed to monitor River temperatures, salinities, and currents at various locations in the River from 20.9 mi south of IPEC (downstream) to 9.5 mi north of IPEC (upstream) during a 10-week period from 5 July through 10 September 2010. These data were analyzed, along with other publicly available River and meteorological observations, to first assess the dynamics of the thermal plume resulting from the IPEC discharge, and then to understand the response of the plume to various environmental forcing factors, such as tides, water temperature, salinity and currents, as well as meteorological conditions that substantially affect thermal regimes.

The long term, fixed mooring field program used a extensive number of thermistors (i.e., 348 thermistors on 66 moorings) to characterize the thermal structure in the River in the extended vicinity of IPEC discharge, accounting for the fact that the River's thermal structure varies with location, as well as with seasonal, daily, and tidal time scales. In addition, the current data from three fixed ADCPs, at Stony and Indian Points, and Iona Island, captured the physical dynamics – including velocity and water elevation over time -- in this area, which also influence the thermal regime. A series of eight CTDs acquired salinity data in the vicinity of the ADCPs, three near bottom and one near surface. The relative contributions of different forcing mechanisms, including River flow, tide and salt-induced estuarine circulation, cause temporal and spatial variability of the flow patterns. In general, bi-directional tidal flow with a period of 12.42 hours is dominant. The combined effect of River flow and salt intrusion resulted in estuarine circulation, where the surface flow was stronger during ebb while the bottom flow was stronger during flood. Also, the distinctive signal of the bi-weekly spring-neap cycle was observed. The 2010 data represented conditions that approached the extreme environmental conditions during August 2005 identified in Swanson et al. (2010b), particularly the water temperatures during July.

6.2 MODEL RESULTS

A model validation effort was performed using both qualitative and quantitative methods that represent the industry standard, providing confidence in model results. The approach used is described in detail in Swanson et al. (2010b) and the standards in McCutcheon et al. (1990) and Warner et al. (2005). The parameters that were evaluated in the model calibration phase were water surface elevations, currents and temperatures. Specifically, the time series of observations vs. model predictions showed that the model captured both the surface elevation and currents variations with respect to phase and amplitude. The model was able to successfully simulate the current velocities with respect to the important tidal signals in the River including semi-diurnal, bi-directional flow, diurnal inequality and the bi-weekly spring-neap cycle. Most importantly, the model was able to reproduce the spatial and temporal variation in River temperature.

The comparison of the model predicted surface and bottom temperatures to the observations on both a qualitative (time series and plume transport map plots) and quantitative basis (statistics analysis) showed that the model adequately predicts the location and spatial dynamics of the plume, the key quantities necessary for the assessment of the regulatory thermal criteria.

The statistical parameters used in the analysis include: relative mean error (RME), error coefficient of variance (ECV), and squared correlation coefficient, r^2, and Skill.

Table 6-1 summarizes the averaged statistical metrics for the three independent parameters, water surface elevation, current velocities, and temperature, for the 8 through 30 July validation period. Those metrics that were met are shown with bolded font. The summary shows that the model did well at achieving the goal metrics with the water surface elevation meeting all four guidance values; the current velocities met three of the guidance values and came close to the fourth; and, most importantly, the temperature met two guidance values and did adequately on the other two. The temperature RME and ECV values are much smaller than the guidance levels, implying that the model predicts the water temperatures well. On average, the skill level of 0.74 is less than the guidance level of 0.85, but is highly dependent on the timing of the compared signals. In addition, the range of temperature variation for the 2010 modeling period was smaller than the calibration period (Swanson et al., 2010b) and thus the variance and standard deviation were smaller, which resulted in relatively lower values for the squared correlation coefficients and skill.

Table 6-1. Model averaged statistics summary for the 8 through 30 July period.

Parameter	RME (%)	RME Goal	ECV (%)	ECV Goal	R^2	R^2 Goal	Skill	Skill Goal
Water Surface Elevation	**1.5**	<30	**0.2**	<10	**0.97**	>0.94	**0.97**	>0.99
Current Velocity	**6.9**	<30	**1**	<10	0.89	>0.94	**0.95**	>0.92
Temperature	**0.5**	< ±25	**1.3**	<45	0.59	>0.84	0.74	>0.85

Table 6-2 presents summary of the averaged statistical metrics for the 2009 calibration period (Swanson et al., 2010b). The summary shows that the model did well at achieving the goal metrics with the water surface elevation meeting three guidance values and only slightly exceeded the fourth; the current velocities met two of the guidance values and slightly exceeded two; and the temperature met three of four guidance values. Those metrics that were met are shown with bolded font.

Table 6-2. Model averaged statistics summary for the calibration period (Swanson et al., 2010b).

Parameter	RME (%)	RME Goal	ECV (%)	ECV Goal	R^2	R^2 Goal	Skill	Skill Goal
Water Surface Elevation	**3**	<30	**9**	<10	0.90	>0.94	**0.96**	>0.85
Current Velocity	**6**	<30	14	<10	0.83	>0.94	**0.93**	>0.92
Temperature	**3**	<25	**3**	<45	**0.87**	>0.84	0.78	>0.85

It should be noted, that a model validation does not typically have the same level of statistical comparison between model results and observations as a model calibration since the tuning of the model during the calibration process is only to the calibration data set. In this case however, the model application to the validation time period was as good or better than the majority of the statistical

measures calculated for the calibration application. This comparison clearly shows that the model is capable of predicting observations on an independent data set of a different season than the calibration data set. It also shows that the model is adequate and sufficient for the evaluation of the IPEC thermal plume dynamics in relation its compliance with the thermal criteria.

6.3 Comparison To Thermal Criteria

The model temperature results for the 8 through 30 July period were post-processed to determine if the IPEC thermal discharge was in compliance with NYSDEC Thermal WQS. The first analysis of the results consisted of determination of any occurrence of water temperature in the estuary (beyond the inferred mixing zone) greater than 90°F, the maximum allowable per the WQS outside a defined mixing zone.

The results of the 90°F analysis showed that the variation of the surface area coverage of the 90°F was predominantly semi-diurnal (tidally driven), and averaged 2.2 ac over the simulation. There were two short term events seen in the record, which peaked at 14.6 ac. These peaks occurred during early ebb tide when the slack water pooling of warmer waters at the outfall was carried downstream Most of the peaks were between 4 ac and 5 ac in size while a smaller set ranged between 5 and 14 ac. These areas are smaller than the 2005 extreme environmental condition results (Swanson et al., 2010b) which found a maximum area of under 35 ac and was typically less than 20 ac. The plume is restricted to the near surface, and does not appear to extend beyond the inferred mixing zone.

The 8 through 30 July 2010 period results were processed to determine the natural ambient temperature close to the plant. Following the procedure described in the earlier modeling report (Swanson et al., 2010b) the model was run with no thermal discharges from any plant. The thermistor station 27 location was used as a proxy for the ambient temperature. The surface ambient temperature reached a maximum of 82.2°F, always under the 83°F threshold where the allowable plume temperature rise is limited to 1.5°F versus the 4°F. Therefore, only the spatial extent of the cross sectional area and surface width of the 4°F were calculated to determine compliance.

The 4°F ΔT analysis showed that the surface width and vertical cross section area percentages generally repeated with tidal cycle regularity at all of the nine transects analyzed. The results for vertical cross section area showed that the maximum extent was 7.8% of the River vertical cross section area with other transects showing maximum percentages from 0.5 to 7.1%, exclusive of the northernmost and southernmost transects which saw no areas greater than zero at 4°F ΔT. These results are well below the Thermal WQS cross section area limit of 50%.

The results for surface width showed that the maximum extent was 23.9% of the River surface width with other transects showing maximum percentages from 5 to 22%, exclusive of the northernmost and southernmost transects which saw no width greater than zero at 4°F ΔT. These results are well below the Thermal WQS surface width limit of 67%.

In conclusion, a second triaxial study was conducted in summer 2010 following one in late summer / early fall in 2009 (Swanson et al., 2010b). The field program each year mapped the extent of the thermal plume from IPEC and was used to calibrate (2009 data) and validate (2010 data) a numerical model representing the study area. The successfully calibrated and validated model was used determine that IPEC was in compliance with NYSDEC Thermal WQS.

7 REFERENCES

Central Hudson Gas and Electric Co., Consolidated Edison Co. of NY, New York Power Authority, and Southern Energy New York, 1999. Draft Environmental Impact Statement for State Pollutant Discharge Elimination System Permits for Bowline Point, Indian Point 2 & 3, and Roseton Steam Electric Generating Stations. Prepared for New York State Department of Environmental Conservation.

LMS , 2005, Danskammer Point Generating Station Tri-Axial Thermal Survey Outfalls 002, 003, and 004. Prepared by Lawler, Matusky and Skelly Engineers LLP. Prepared for Dynegy Northeast Generation, Inc.

McCutcheon, S.C., Z. Dongwei and S. Bird, 1990. Model calibration, validation, and use. Chapter 5 in: Technical Guidance Manual for Performing Waste Load Allocations, Book III: Estuaries. Part 2: Application of Estuarine Waste Load Allocation Models. Edited by J.L. Martin, R.B. Ambrose and S.C. McCutcheon. United States Environmental Protection Agency, Office of Water. March 1990.

Swanson, C.,Y. Kim, D. Mendelsohn, D. Crowley, and M. Mattson, 2010a, Preliminary Analysis of Hudson River Thermal Data, ASA report #09-167-1. South Kingstown, RI. Prepared for Elise Zoli, Goodwin Proctor, Boston, MA.

Swanson, C.,Y. Kim, D. Mendelsohn, and D. Crowley, 2010b. Hydrothermal Modeling of the Cooling Water Discharge from the Indian Point Energy Center to the Hudson River, ASA report #09-167-2. South Kingstown, RI. Prepared for Elise Zoli, Goodwin Proctor, Boston, MA.

Swanson, C.,Y. Kim, D. Mendelsohn, and D. Crowley, 2010c. Response to the NYSDEC CWA § 401 Water Quality Certification Notice of Denial Related to Thermal Discharges at Indian Point. ASA report #09-167-3. South Kingstown, RI. Prepared for Elise Zoli, Goodwin Proctor, Boston, MA.

Texas Instruments, November 1976. A Synthesis of Available Data Pertaining to Major Physicochemical Variables within the Hudson River Estuary Emphasizing the Period from 1972 to 1975. New York, NY: Prepared for Consolidated Edison Company of New York, Inc. Prepared by Texas Instruments Incorporated Ecological Services.

Warner, J., W. Geyer, and J. Lerczak. 2005. Numerical modeling of an estuary: A comprehensive skill assessment. Journal of Geophysical Research, v. 110.